A petrological and geochemical study of the volcanic rocks of the Crowsnest Formation, southwestern Alberta, and of the Howell Creek suite, British Columbia

Melissa Bowerman, Amy Christianson, Robert A. Creaser, and Robert W. Luth

Abstract: Alkaline igneous rocks of the Crowsnest Formation in southwestern Alberta and in the Howell Creek area in southeastern British Columbia have been suggested previously to be cogenetic. To test this hypothesis, samples of both suites were characterized petrographically and their major and trace element geochemistry was determined. A subset of the samples was analyzed for whole-rock Sr and Nd isotope geochemistry. The samples of the two suites are latites, trachytes, and phonolites based on the International Union of Geological Sciences (IUGS) total alkalis versus silica (TAS) diagram. Samples from both suites show similar patterns on mantle-normalized trace element diagrams, being enriched relative to mantle values but depleted in the high field-strength elements Nb, Ta, and Ti relative to the large-ion lithophile elements. The chondrite-normalized rare-earth element (REE) patterns for both suites are light REE enriched, with no Eu anomaly and flat heavy REE. The isotope geochemistry of both suites is characterized by low initial ^{87}Sr/^{86}Sr (Sr_T = 0.704 to 0.706) and low εNd_T (–7 to –16). The Howell Creek samples have lower εNd_T and higher Sr_T than do the Crowsnest samples. Based on the intra- and intersuite differences in the isotope geochemistry, we conclude that these samples are not cogenetic, but rather represent samples that have experienced similar evolutionary histories from a heterogeneous source region in the subcontinental lithospheric mantle.

Résumé : Les roches ignées alcalines de la Formation de Crowsnest dans le sud-ouest de l’Alberta et dans le secteur du ruisseau Howell dans le sud-est de la Colombie-Britannique étaient antérieurement considérées cogénétiques. Afin de vérifier cette hypothèse, des échantillons des deux suites ont été caractérisés pétrographiquement et la géochimie des éléments majeurs et des éléments traces a été déterminée. Un sous-ensemble des échantillons a été analysé pour la géochimie des isotopes Sr et Nd sur la roche entière. Selon le diagramme TAS (« Total Alkalis vs. Silica ») de l’IUGS comparant les alcalins et la silice, les échantillons des deux suites sont des latites, des trachytes et des phonolites. Les échantillons des deux suites présentent des patrons semblables sur les diagrammes d’éléments traces normalisés pour le manteau, étant enrichis par rapport aux valeurs du manteau mais appauvris en éléments à forte électronégativité Nb, Ta et Ti par rapport aux éléments lithosphériques à grand rayon ionique. Dans les deux suites, les patrons des éléments de terres rares (REE) normalisés pour la chondrite sont enrichis en éléments des terres rares légères (LREE), sans anomalie Eu et les teneurs en éléments de terres rares lourdes (HREE) sont uniformes. La géochimie des isotopes des deux suites est caractérisée par des rapports initiaux ^{87}Sr/^{86}Sr (Sr_T = 0,704 à 0,706) faibles ainsi que des valeurs εNd_T faibles (–7 à –16). Les échantillons du ruisseau Howell ont des valeurs εNd_T inférieures et des valeurs Sr_T supérieures à celles des échantillons Crowsnest. En se basant sur les différences intra- et inter-suite de la géochimie des isotopes, nous concluons que ces échantillons ne sont pas cogénétiques, mais qu'ils représentent plutôt des échantillons qui ont subi des historiques évolutionnaires similaires à partir d’une région source hétérogène dans le manteau subcontinental lithosphérique.

[Traduit par la Rédaction]

Introduction

Since the work of Price (1959, 1962), there have been repeated attempts to determine if different suites of alkalic igneous rocks of Cretaceous age in southeastern British Columbia and southwestern Alberta (Fig. 1) are genetically related (Goble et al. 1993; Peterson et al. 1997; Goble et al. 1999; Barnes 2002). Of these suites, the best known and most studied are the volcanic rocks of the Crowsnest Formation, which are exposed in thrust fault-bounded slices in the Front

Received 14 June 2005. Accepted 21 March 2006. Published on the NRC Research Press Web site at http://cjes.nrc.ca on 5 January 2007.

Paper handled by Associate Editor J. Greenough.

M. Bowerman, A. Christianson,[1] R.A. Creaser, and R.W. Luth.[2] Department of Earth and Atmospheric Sciences, University of Alberta, Edmonton, AB T6G 2E3 Canada.

[1] Present address: Department of Geological Sciences, University of Canterbury, PB 4800, Christchurch, New Zealand.
[2] Corresponding author (e-mail: robert.luth@ualberta.ca).

Can. J. Earth Sci. **43**: 1621–1637 (2006) doi:10.1139/E06-037

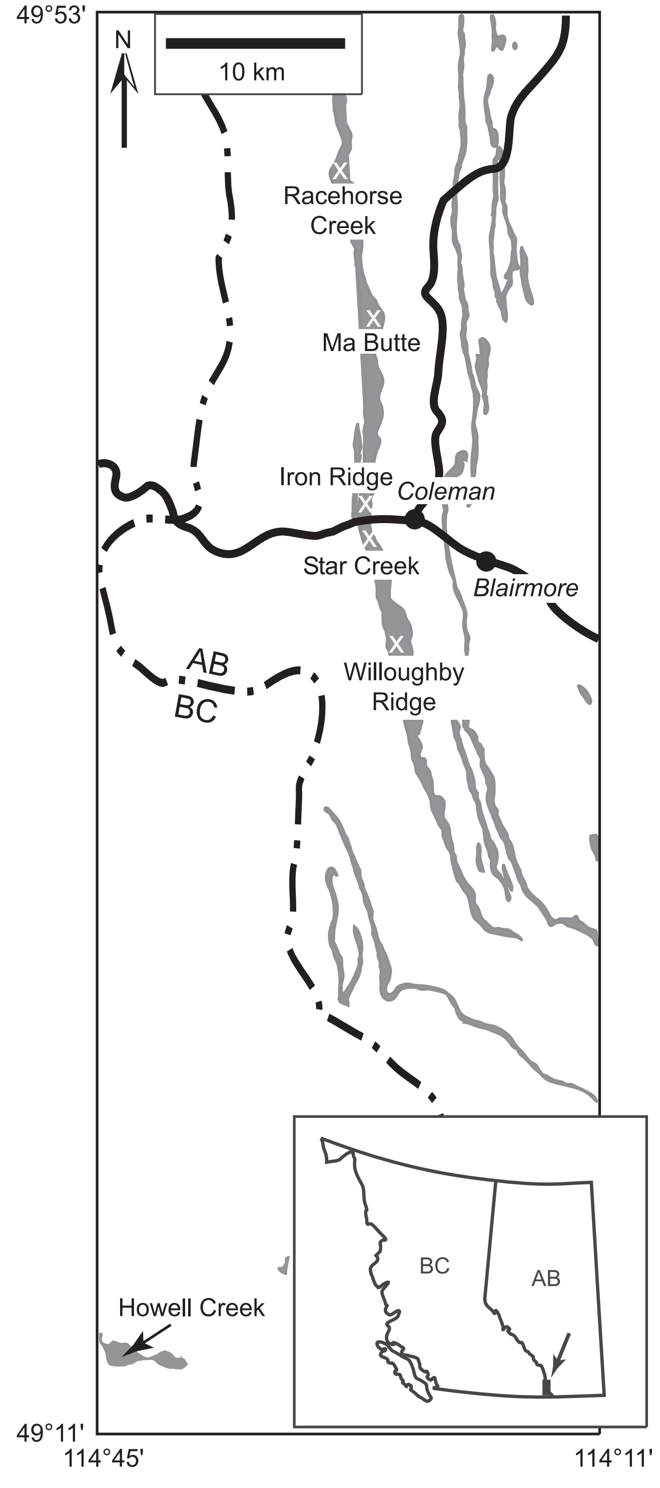

Fig. 1. Map of southeastern British Columbia and southwestern Alberta. Gray shaded areas are the outcrop of the Crowsnest Formation and the Howell Creek intrusive suite, after Price (1962). Heavy solid line running east–west is Highway 3; heavy dot-dash line is the Alberta – British Columbia border. Specific localities for samples of the Crowsnest volcanics are indicated on the figure. Inset map shows approximate location of area relative to the provincial borders of British Columbia and Alberta.

Ranges of the southern Alberta Rockies, in and around the Crowsnest Pass area. Originally described by Dawson (1886), these rocks have generated interest and controversy, in part because of the presence of analcime ($NaAlSi_2O_6 \cdot H_2O$) as apparent phenocrysts in some of the volcanic units. Analcime could precipitate from a hydrous melt, or it could form by hydration and ion exchange of primary leucite phenocrysts. Other unusual characteristics of the volcanics include the presence of Ti-rich schorlomite and Fe^{3+}-rich clinopyroxene, and the absence of any hydrous ferromagnesian mineral.

The primary goal of this study is to compare the Crowsnest volcanics and the Howell Creek Intrusive Suite based on major and trace element whole-rock geochemistry, and on Rb–Sr and Sm–Nd isotope geochemistry in an attempt to establish an unequivocal relationship between the two suites. Additional goals were to provide new insight into the petrogenesis of the two suites, and to determine the relationship among the volcanics of different composition within the Crowsnest suite.

Regional geology

Crowsnest Formation

The Crowsnest Formation forms the upper part of the nonmarine, Early Cretaceous Blairmore Group of southern Alberta and British Columbia. The contact between the Crowsnest Formation and the sedimentary formations of the Blairmore Group is gradational, with volcanic fragments becoming progressively more common towards the top of the middle Blairmore Group (Norris 1964). The Crowsnest Formation, comprising volcanic and epiclastic rocks, is unconformably overlain by the shales of the Blackstone Formation that were deposited during a marine transgression in the Late Cretaceous (Norris 1964). The age of the Crowsnest Formation is ~100 Ma, based on radiometric age dating and faunal studies (cf. review in Peterson et al. 1997). The current location of the Crowsnest Formation (Fig. 1) is a result of the subsequent deformation and thrust faulting in the southern Canadian Rocky Mountains; palinspastic reconstruction places the original location ~75 km west (Norris 1964).

Howell Creek

The Howell Creek suite comprises numerous small hypabyssal and intrusive bodies in southeastern British Columbia, ~45 km south-southwest of the outcrops of the Crowsnest volcanics studied in this project (Fig. 1). The area in which the Howell Creek suite crops out is bounded by faults, but both the orientation and sense of movement on the faults are controversial (cf. summary by Barnes 2002). For the purposes of the present study, the major conclusion is that the original position of the Howell Creek suite was < 100 km to the southwest of its present position (Barnes 2002). Ar–Ar age determinations by Barnes (2002) on samples from the same localities as studied here yield ages of ~102 Ma.

Methods

Field work

Samples were collected during the summer of 2002, with the goal of obtaining representative samples of both the Crowsnest volcanics and the Howell Creek suite. The sampling of the Howell Creek localities was guided by E. Barnes, with the goal of obtaining samples with the least amount of hydrothermal alteration. Sample locations are detailed in Table 1, and the localities for the Crowsnest samples are shown in Fig. 1.

Petrography

The phenocryst mineralogy of the samples, as observed in hand sample and thin section, is summarized in Table 2. In all samples, the feldspars have varying degrees of alteration (sericitization and albitization), whereas the pyroxenes and garnets (if present) are not altered. Variable degrees of alteration of the analcime were observed, as noted by previous workers (Pearce 1967, 1970; Peterson et al. 1997). The matrix in the samples consisted of feldspar ± chlorite with variable amounts of optically unresolvable material. Barnes (2002) described her samples of the Howell Creek suite as intrusive, but the fine-grained nature of the matrix of these samples is certainly permissive of classifying these rocks based on the total alkalis versus silica (TAS) diagram of Le Maitre (2002) to facilitate comparison with the Crowsnest samples. The intrusive names as used by Barnes (2002) are noted in the footnote of Table 1.

Whole-rock major and trace element geochemistry

Selected samples were trimmed to remove weathered surfaces and crushed in a steel jaw crusher. Aliquots of each were powdered in steel and tungsten carbide shatterboxes. Splits of each sample were sent to Activation Laboratories Ltd. of Ancaster, Ontario, where they were analyzed by ICP (inductively coupled plasma) for major elements and ICP–MS (ICP – mass spectrometry) for trace elements. Estimated accuracy of the analyses, based on analyses of standards by Activation Laboratories Ltd., are listed in the footnote to Table 1.

Radiogenic isotope geochemistry

Sm–Nd and Rb–Sr isotopic analyses on aliquots of selected samples were performed at the Radiogenic Isotope Facility at the University of Alberta. Sample powders were weighed, totally spiked with known amounts of mixed ^{84}Sr–^{87}Rb and ^{149}Sm–^{150}Nd tracers, and then Rb, Sr, Sm, and Nd were separated by conventional ion-chromatography techniques (Holmden et al. 1996; Creaser et al. 1997). Determinations of Rb, Sr, and Sm abundances and Sr isotopic composition were made by isotope-dilution mass spectrometry using a Micromass Sector 54 thermal ionization mass spectrometer (TIMS). The long-term value for the SRM987 Sr isotopic standard determined by TIMS is 0.71026 ± 0.00002 (1 SD (standard deviation)). Neodymium isotope analysis was made using a NuPlasma multicollector ICP mass spectrometer (MC-ICP–MS). An in-house Nd isotopic standard with a known value relative to the La Jolla Nd isotope standard was measured along with the samples and was used for normalization. The Sr and Nd isotope data reported here are presented relative to values of 0.710245 for SRM987 and 0.511850 for the La Jolla Nd isotopic standard.

Results

The rocks are all alkalic, plotting dominantly in the trachyandesite (latite), phonolite, and trachyte fields of the International Union of Geological Sciences (IUGS) TAS diagram (Fig. 2). The single phonotephrite has very high CaO and loss on ignition (LOI) contents (Table 1), consistent with the extensive secondary calcite precipitation seen in thin section. Therefore, the geochemistry of this sample is excluded from subsequent diagrams and discussion. The only noticeable differences in the samples processed in the tungsten carbide and steel shatterboxes were enrichments in Co and W in samples from the former (not tabulated).

Although all of the samples could be termed “high-K,” most are not ultrapotassic (i.e., molar K_2O/Na_2O tends to be < 3), and most are metaluminous rather than peralkaline (Table 1). The high silica and alkali contents relative to total iron and MgO result in the samples plotting near the alkali apex of an alkali–FeO–MgO (AFM) diagram.

The Crowsnest samples show crude negative correlations of Fe_2O_3*, MgO, TiO_2, and CaO with SiO_2 and a positive correlation of Al_2O_3 with SiO_2 (CaO and Al_2O_3 illustrated in Fig. 3). The K_2O–SiO_2 and Na_2O–SiO_2 diagrams (Fig. 3) show more scatter, possibly resulting from multiple superimposed trends or the effects of alteration as discussed later in the text. The variation diagram for P_2O_5 shows a cluster of high-P_2O_5 samples at low SiO_2 that are offset to higher P_2O_5 values from the rest of the samples, which have a trend that slightly decreases in P_2O_5 with increasing SiO_2 content (Fig. 3). The data for the Howell Creek samples are limited by the paucity of samples (Fig. 3), with the phonolites and trachytes plotting in different clusters.

Trace element variations with SiO_2 for the Crowsnest suite show variable trends: Mn decreases with increasing SiO_2 (not shown), La concentrations show a negative trend at higher SiO_2 concentrations (Fig. 3), whereas Lu and Zr show no trend (Fig. 3). The trace element concentrations for the Howell Creek trachytes and phonolites differ from one another (Fig. 3). The trace element concentrations of all samples are enriched relative to primitive mantle values (Fig. 4). All samples have enrichments in K, Pb, and Sr, and depletions in Nb, Ta, P, and Ti relative to neighbouring elements. There is no systematic variation in the concentrations of trace elements among the different rock types in the Crowsnest suite, but the Howell Creek phonolites tend to have higher trace element concentrations than do the trachytes (Fig. 4*b*). The Howell Creek samples have similar “sawtooth” patterns to those from the Crowsnest; the only notable difference is the higher Th concentrations in the Howell Creek phonolites.

The patterns of the chondrite-normalized rare-earth element (REE) concentration for the Crowsnest suite (Fig. 5*a*) are Light REE (LREE)-enriched, with no Eu anomalies and flat heavy REE (HREE) concentrations, consistent with the findings of Peterson et al. (1997). The samples of the Howell Creek suite have similar REE patterns to those of the Crowsnest samples, with enriched LREE and flat HREE concentrations relative to chondritic values and no Eu anomalies (Fig. 5*b*). The Howell Creek samples differ from the Crowsnest suite, however, in having greater variability in their LREE concentrations, with the phonolites having higher concentrations than do the trachytes. The Howell Creek trachytes have patterns parallel to those of the Crowsnest trachytes but offset to lower concentrations. In contrast, the Howell Creek phonolites have similar LREE concentrations to the Crowsnest phonolites,

Table 1 (*runs from p. 1624 to p. 1626*) Whole-rock geochemistry

	Crowsnest										
Sample:	MCN02-44	MCN02-45	MCN02-13	MCN02-4	MCN02-5	MCN-9	MCN02-38	MCN02-39	MCN-39	MCN02-24	MCN02-25
Rock type:	TA	PT	T	T	P	T	P	P	TA	T	T
Location:	RCN	RCN	RCS	MB	MB	IR	SC	SC	PC	WR	WR
Easting:	675931	675931	675348	677552	677552	677832	677832	677832	678370	680681	680681
Northing:	5519637	5519637	5519433	5509749	5509749	5500674	5499498	5499498	5499856	5490432	5490432
Major elements (wt.%)											
SiO_2	53.37	40.56	60.87	59.75	57.67	58.57	54.54	62.61	55.27	59.48	59.46
Al_2O_3	15.50	14.09	20.22	19.57	16.46	18.16	18.43	18.18	16.17	17.84	17.35
$Fe_2O_3{}^T$	7.81	3.56	3.08	3.77	3.47	4.40	5.81	1.52	6.89	4.86	5.18
MnO	0.17	0.59	0.10	0.12	0.19	0.14	0.14	0.02	0.23	0.16	0.21
MgO	1.49	0.56	0.30	0.24	0.38	0.56	0.70	0.11	1.50	0.61	0.68
CaO	4.62	14.76	1.00	1.80	4.36	3.10	1.83	0.52	4.48	2.61	2.39
Na_2O	1.48	3.27	7.19	6.74	2.11	5.02	3.94	1.76	1.98	4.59	4.51
K_2O	7.35	5.86	4.27	4.66	10.77	6.54	7.74	12.99	8.59	7.25	6.90
TiO_2	0.61	0.54	0.22	0.37	0.32	0.56	0.64	0.48	0.81	0.59	0.54
P_2O_5	0.10	0.09	0.05	0.08	0.06	0.09	0.09	0.05	0.27	0.10	0.09
LOI	7.04	14.98	2.21	2.26	3.51	2.09	4.89	1.22	3.13	1.56	1.58
Total	99.54	98.87	99.50	99.36	99.29	99.22	98.75	99.46	99.32	99.65	98.89
ASI	MAL	MAL	PAL	MAL	MAL	PAL	PAL	PAL	MAL	MAL	MAL
Trace elements (ppm)											
Ba	2528	3073	1302	2287	3107	2387	3940	2602	2712	1950	1951
Sr	1074	1517	2845	3555	2210	2728	1628	854	2741	3884	3941
Zr	149	166	283	261	206	230	214	157	263	215	183
Rb	149	110	139	106	298	202	222	239.7	214.4	183.6	140.4
Y	6.45	11.0	12.1	16.9	9.47	20.9	11.4	6.20	15.5	21.8	20.6
Nb	25.7	24.8	37.9	25.4	33.7	30.9	48.0	33.2	37.1	30.8	29.2
Cs	3.82	5.97	7.78	8.22	2.67	6.34	18.0	0.62	3.60	2.63	1.00
La	43. 8	42.1	47.7	62.0	70.7	64.8	55.9	32.6	67.9	64.8	59.3
Ce	79.0	72.5	80.0	109	117	118	103	64.8	123	113	102
Pr	8.46	7.69	8.39	11.1	10.2	12.0	10.4	6.44	12.9	11.9	10.8
Nd	30.2	28.3	27.3	38.9	30.1	44.2	34.7	21.0	46.9	44.2	40.0
Sm	4.32	4.52	3.75	5.94	3.45	7.26	4.63	2.68	7.69	7.30	6.70
Eu	1.24	1.23	1.19	1.85	1.04	2.23	1.24	0.69	2.33	2.14	1.95
Gd	3.26	3.25	2.70	4.50	2.51	6.20	3.02	1.86	5.68	5.70	4.99
Tb	0.33	0.41	0.36	0.60	0.29	0.80	0.37	0.20	0.67	0.75	0.67
Dy	1.37	1.93	1.93	3.11	1.45	4.07	1.91	0.98	3.18	3.91	3.48
Ho	0.20	0.33	0.38	0.59	0.28	0.76	0.33	0.17	0.55	0.71	0.66
Er	0.62	0.96	1.20	1.77	0.86	2.26	0.99	0.57	1.53	2.04	1.85
Tm	0.07	0.15	0.18	0.28	0.13	0.35	0.16	0.08	0.22	0.31	0.28
Yb	0.48	0.91	1.27	1.77	0.85	2.20	1.12	0.56	1.50	1.99	1.79
Lu	0.07	0.13	0.20	0.26	0.13	0.31	0.17	0.09	0.22	0.31	0.28
Ta	1.09	0.92	1.29	1.17	1.07	1.75	1.95	1.46	2.97	1.85	1.64
Pb	22	14	24	26	21	16	23	15	20	21	12
Th	14.9	13.0	15.4	12.8	16.9	14.1	15	8.28	15.3	15.0	13.8
U	10.6	3.45	2.01	3.06	15.0	1.84	3.91	4.36	7.47	1.83	1.17
Isotopic data											
Rb	143.5	111.1	137.1	107.7	286.5		242.1	222.8		196.8	148.2
Sr	1052	1417	2831	3455	2050		1735	818.7		4265	3726
$^{87}Rb/^{86}Sr$	0.3947	0.2269	0.1401	0.0902	0.4043		0.4036	0.7875		0.1335	0.1151
$^{87}Sr/^{86}Sr$	0.705207	0.704930	0.704522	0.704556	0.704961		0.704780	0.705306		0.704679	0.704672
±2 SD	0.000013	0.000017	0.000017	0.000013	0.000013		0.000018	0.000016		0.000014	0.000018
Sr_T	0.704646	0.704607	0.704323	0.704428	0.704387		0.704207	0.704187		0.704489	0.704508
Sm	3.56	4.55	3.85	6.26	3.40		4.89	3.00		7.53	8.40
Nd	24.49	29.23	28.83	40.92	29.67		37.37	23.79		45.47	50.64
$^{147}Sm/^{144}Nd$	0.0879	0.0941	0.0808	0.0925	0.0694		0.0791	0.0761		0.1002	0.1003
$^{143}Nd/^{144}Nd$	0.512115	0.512090	0.511965	0.511965	0.512024		0.512135	0.512180		0.512082	0.512074
±2 SD	0.000007	0.000009	0.000005	0.000008	0.000007		0.000005	0.000006		0.000007	0.000008
T_{DM}	1.27	1.37	1.37	1.50	1.20		1.16	1.09		1.45	1.46
ε_{Nd}(100 Ma)	–8.8	–9.4	–11.7	–11.8	–10.4		–8.3	–7.4		–9.6	–9.8

Table 1. (*continued*).

	Crowsnest							Howell Creek
Sample:	MCN02-28	MCN02-29	MCN02-30	MCN02-32	MCN02-33	MCN02-34	MCN02-35	AB02-01
Rock type:	T	T	TA	TA	TA	TA	TA	T
Location:	WR	WR	WR	WR	WR	WR	WR	
Easting:	680681	680681	680681	680681	680681	680681	680681	667342
Northing:	5490432	5490432	5490432	5490432	5490432	5490432	5490432	5453101
Major elements (wt.%)								
SiO_2	59.57	57.97	56.22	56.15	56.61	56.25	55.75	59.85
Al_2O_3	17.65	17.77	16.07	16.37	16.21	16.26	15.93	17.80
$Fe_2O_3^T$	4.87	5.12	7.82	7.24	6.96	7.27	7.74	3.34
MnO	0.17	0.17	0.28	0.28	0.23	0.28	0.31	0.10
MgO	0.64	0.67	1.32	1.20	1.26	1.19	1.33	0.36
CaO	2.87	3.25	4.97	5.12	4.13	5.09	5.01	3.18
Na_2O	4.53	4.39	3.60	3.91	3.85	3.96	3.41	5.37
K_2O	7.09	7.30	6.85	6.50	7.21	6.60	6.87	5.89
TiO_2	0.65	0.58	0.92	0.91	0.88	0.90	0.96	0.30
P_2O_5	0.11	0.09	0.27	0.25	0.26	0.26	0.28	0.09
LOI	1.45	1.96	1.62	1.73	1.97	1.48	1.65	3.13
Total	99.60	99.28	99.95	99.66	99.58	99.54	99.23	99.41
ASI	MAL	MAL	MAL	MAL	MAL	MAL	MAL	MAL
Trace elements (ppm)								
Ba	1777	1728	1491	1646	1611	1752	1453	2446
Sr	3984	3464	2749	2693	2591	3013	2863	2086
Zr	264	276	206	210	176	210	221	123
Rb	173.3	205.2	224.4	209.2	160.6	206.6	224.8	136.6
Y	25.2	21.2	25.8	26.2	23.4	26.0	26.5	13.0
Nb	34.4	33.8	28.4	27.8	23.2	25.5	27.4	14.4
Cs	1.61	2.92	6.00	4.71	3.60	4.74	5.08	5.06
La	68.1	69.7	68.4	64.2	57.2	60.7	60.9	33.9
Ce	125	120	128	120	110	114	119	61.8
Pr	13.0	12.6	14.2	13.5	12.4	12.8	13.7	6.43
Nd	47.9	45.1	55.2	52.5	47.8	50.0	52.9	22.8
Sm	8.30	7.36	10.0	9.76	8.73	9.22	9.70	3.75
Eu	2.42	2.13	2.90	2.77	2.56	2.68	2.86	1.25
Gd	6.27	5.81	7.93	7.61	6.97	7.09	7.59	3.25
Tb	0.84	0.75	1.03	1.02	0.90	0.97	1.00	0.42
Dy	4.44	3.84	5.17	5.06	4.57	5.01	5.10	2.25
Ho	0.83	0.72	0.92	0.92	0.82	0.89	0.93	0.43
Er	2.38	2.06	2.62	2.55	2.31	2.48	2.60	1.29
Tm	0.36	0.31	0.41	0.38	0.33	0.38	0.39	0.20
Yb	2.27	1.98	2.45	2.35	2.09	2.38	2.44	1.36
Lu	0.36	0.30	0.36	0.36	0.32	0.36	0.38	0.21
Ta	2.03	1.89	1.83	1.80	1.62	1.75	1.88	0.75
Pb	28	20	15	18	19	23	18	19
Th	15.1	15.1	13.6	13.1	12.3	13.8	14.8	10.08
U	3.71	5.73	1.70	2.95	2.75	2.97	2.14	5.14
Isotopic data								
Rb		192.7				213.6	218.6	136.7
Sr		3307				3189	2860	2126
$^{87}Rb/^{86}Sr$		0.1686				0.1939	0.2211	0.1860
$^{87}Sr/^{86}Sr$		0.704724				0.704859	0.704859	0.704829
±2 SD		0.000019				0.000013	0.000015	0.000018
Sr_T		0.704484				0.704584	0.704544	0.704565
Sm		7.35				9.46	11.09	3.90
Nd		44.91				52.86	61.73	24.07
$^{147}Sm/^{144}Nd$		0.0989				0.1082	0.1086	0.0980
$^{143}Nd/^{144}Nd$		0.512007				0.512021	0.512064	0.511877
±2 SD		0.000006				0.000006	0.000007	0.000007
T_{DM}		1.53				1.65	1.59	1.69
ε_{Nd}(100 Ma)		–11.1				–10.9	–10.1	–13.6

Table 1 (*continued*).

	Howell Creek			
Sample:	AB02-03	AB02-04	AB02-07	AB02-09
Rock type:	T	T	P	P
Location:				
Easting:	667342	667342	671040	671040
Northing:	5453101	5453101	5454142	5454142
Major elements (wt.%)				
SiO_2	59.98	58.58	58.22	58.02
Al_2O_3	17.75	17.67	19.37	19.39
$Fe_2O_3^T$	3.46	3.77	2.12	2.08
MnO	0.10	0.09	0.06	0.07
MgO	0.65	0.79	0.32	0.34
CaO	3.16	3.56	0.57	0.57
Na_2O	5.53	5.68	6.80	6.82
K_2O	5.68	4.44	8.16	8.20
TiO_2	0.33	0.28	0.17	0.17
P_2O_5	0.10	0.16	0.02	0.02
LOI	3.23	4.71	3.90	4.07
Total	99.97	99.73	99.71	99.75
ASI	MAL	MAL	PAK	PAK
Trace elements (ppm)				
Ba	2107	2324	1881	1578
Sr	2028	1035	1296	1878
Zr	136	87	346	336
Rb	127.4	101.1	166.7	164.1
Y	13.5	10.6	12.1	11.8
Nb	14.6	9.29	43.0	46.0
Cs	3.55	3.55	5.13	4.41
La	32.3	17.7	62.4	72.2
Ce	62.6	35.7	90.8	100.7
Pr	6.68	4.07	7.51	8.02
Nd	24.2	15.9	21.2	22.5
Sm	4.00	2.92	2.70	2.71
Eu	1.32	1.20	0.81	0.79
Gd	3.38	2.81	1.89	1.86
Tb	0.44	0.34	0.30	0.29
Dy	2.41	1.84	1.69	1.66
Ho	0.47	0.37	0.36	0.34
Er	1.38	1.10	1.16	1.09
Tm	0.23	0.17	0.20	0.19
Yb	1.45	1.17	1.38	1.28
Lu	0.23	0.18	0.20	0.19
Ta	0.77	0.40	1.39	1.33
Pb	31	12	60	55
Th	10.65	5.17	60.16	76.50
U	5.69	3.64	21.75	21.86
Isotopic data				
Rb		101.8	166.2	161.3
Sr		1054	1299	1838
$^{87}Rb/^{86}Sr$		0.2795	0.3701	0.2540
$^{87}Sr/^{86}Sr$		0.705999	0.705450	0.705278
±2 SD		0.000014	0.000015	0.000016
Sr_T		0.705601	0.704924	0.704917
Sm		3.17	2.76	2.85
Nd		17.11	22.44	45.47
$^{147}Sm/^{144}Nd$		0.1119	0.0743	0.0725
$^{143}Nd/^{144}Nd$		0.512054	0.511742	0.511775
±2 SD		0.000006	0.000007	0.000011
T_{DM}		1.66	1.55	1.50
ε_{Nd}(100 Ma)		–10.3	–15.9	–15.3

Table 1 (*concluded*).

Note: Rock types: T, trachyte; TA, trachyandesite; PT, phonotephrite, P, phonolite. Names are based on IUGS recommendations for volcanic rocks (Le Maitre 2002). Localities: RCN, Racehorse Creek North; RCS, Racehorse Creek South; MB, Ma Butte; IR, Iron Ridge; SC, Star Creek; PC, Pipeline Cut; WR, Willoughby Ridge. Eastings and northings are according to Universal Transverse Mercator (UTM) Zone 11U, North American Datum (NAD)27. $Fe_2O_3^T$, total iron expressed as Fe_2O_3. LOI, loss on ignition. ASI, alumina saturation index (Shand 1927); PAL, peraluminous; MAL, metaluminous; PAK, peralkaline. T_{DM}, depleted mantle model age. Accuracy, as estimated based on analyses of standards (one diabase, one dolerite, two syenites) from Activation Laboratories Ltd.: $Al_2O_3 < 0.2$ wt.%; SiO_2, MgO, CaO, $Na_2O < 0.1$ wt.%; MnO, K_2O, TiO_2, $P_2O_5 < 0.02$ wt.% (all absolute wt.%). Trace elements: < 5% relative: Sr, Y, Sm, Eu, Gd, Yb. < 10% relative: Ba, Zr, Rb, La, Nd, Tb, Dy, Ho, Tm, Lu. Er:13% relative, Cs, Ce, Th, U < 20% relative, Nb 21%, Pr 26%, Pb 38% relative. Sr_T is $^{87}Sr/^{86}Sr$ at 100 Ma. ±2 SD is ±2 standard deviations of the measurement in the preceding line in the table. AB02-01, AB02-03, AB02-04 from same outcrop as EB 1301 (Barnes 2002); AB02-07, AB02-09 from same outcrop as EB 1810. EB1301 and EB 1810 were called megacrystic syenite and foid syenite, respectively, by Barnes (2002).

but higher HREE contents. This difference results in a steeper pattern for the Crowsnest phonolites relative to those for the Howell Creek phonolites.

Initial ε_{Nd} values (εNd_T) for samples from both suites are negative, ranging from –7 to –12 for the Crowsnest samples and –10 to –16 for the Howell Creek samples (Fig. 6). Initial $^{87}Sr/^{86}Sr$ values (Sr_T) are low, with values for the Crowsnest samples below the value for bulk earth at 100 Ma. The Crowsnest samples form a tighter cluster in εNd_T – Sr_T space relative to the more variable Howell Creek samples (Fig. 6), but the variability even in the Crowsnest data cluster is well outside analytical uncertainties, which are less than the size of the symbols in Fig. 6.

Discussion

Intrasuite compositional trends

Before any discussion of the compositional trends of the two suites, the effects of alteration must be considered, especially in light of LOI values > 3 for some samples (Table 1). The Crowsnest Formation has undergone low-grade metamorphism, with maximum temperatures of 180–280 °C and pressures of 0.15 – 0.3 GPa (Bégin et al. 1995*b*). These authors report metamorphic mineral assemblages of vein-forming analcime, vein-forming and pseudomorphic calcite, amygdaloidal prehnite, and pore-filling laumontite. They found the matrix of their samples to contain a mixture of quartz, K-feldspar, albite, and chlorite. To what extent this metamorphism has modified elemental abundances is not clear. Peterson et al. (1997) stated that they found no systematic differences among their samples, which were selected from least-altered samples, and the more altered samples of Bégin et al. (1995*a*). On the other hand, Crook (1962) and Pearce (1970) both report albitization of sanidine in the Crowsnest volcanics, with Pearce (1970) noting that it was developed best in phenocrysts in the trachytes but poorly developed or absent in the analcite-bearing phonolites. Evidence that Na and K may have been mobile during the metamorphism of the Crowsnest rocks may also be seen in the K_2O – Na_2O relationships (Fig. 7). This plot has been used by previous authors to discriminate the differentiation trends of different suites of continental alkaline rocks (e.g., McBirney

Table 2. Phenocryst mineralogy of samples.

Sample	Alkali feldspar	Cpx	Analcime	Garnet
Crowsnest				
MCN02-04	x	x		<1%
MCN02-05	x	x		<1%
MCN-9	x	x		
MCN02-13	x	x		<1%
MCN02-24	x	x		x
MCN02-25	x	x		x
MCN02-28	x	x		x
MCN02-29	x	x		x
MCN02-30	x	x		
MCN02-32	x	x		
MCN02-33	x	x		
MCN02-34	x	x		
MCN02-35	x	x		
MCN02-38	x	x	x	x
MCN02-39				
MCN02-44	x		x	<1%
MCN02-45	x		x	
MCN-39	x	x	x	
MCN-9				
Howell Creek				
All samples	x	x		

Note: Cpx, clinopyroxene.

1993; Winter 2001). The overall trend shown by the Crowsnest samples is normal to these trends, with samples scattering between high K_2O and low Na_2O and between low K_2O and high Na_2O end members. This array is consistent with other recent whole-rock analyses of the Crowsnest volcanics (Bégin et al. 1995*a*; Peterson et al. 1997). The trachytes (field labelled T in Fig. 7) have the highest Na_2O contents in this array, consistent with more pronounced albitization in these rocks (Pearce 1970). It is likely that the alkalis were mobilized during the low-grade metamorphism of this suite, and their concentrations should not be taken as representative of the original igneous concentrations. On the other hand, the high field-strength elements (HFSE) and REE are thought to be immobile — or at least less mobile — in fluids at low-grade conditions (e.g., Pearce and Cann 1973; Floyd and Winchester 1975; Wood et al. 1976; Middelburg et al. 1988).

For the Howell Creek suite, Barnes (2002) examined a larger number of samples with varying degrees of alteration and found that the more extensively altered samples had lower Na and higher K contents relative to the least-altered samples (which were from the outcrops sampled for this study). We cannot rule out, therefore, that these samples have not experienced mobilization of the alkalis.

The scatter in the trends for major and trace elements in the variation diagrams (Fig. 3) consistent with either elemental mobilization during metamorphism or alteration or the possibility that the samples of each suite are not related by fractional crystallization. This latter possibility is supported by the intrasuite differences in εNd_T and Sr_T.

Even the Crowsnest samples, which cluster more tightly than do the Howell Creek samples in εNd_T – Sr_T space (Fig. 6), show variability that is geographically related (Fig. 8). Indeed, even samples from a single locality, Willoughby Ridge, show a range in εNd_T and Sr_T that is well outside analytical uncertainty. Such a range is consistent with assimilation of crustal material into the magma, post-emplacement alteration, or heterogeneities in the source region(s) of the magmas.

Fig. 2. Total alkalis versus silica diagram for Crowsnest (circles) and Howell Creek (triangles) samples. Fields after Le Maitre (2002).

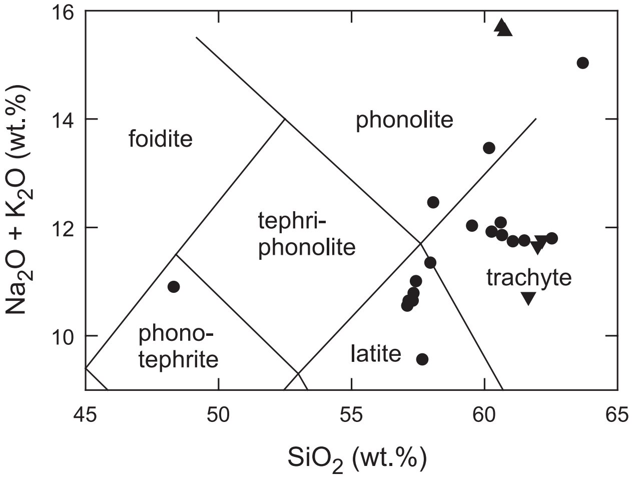

In the absence of samples from the lower crust in the area, average compositions must be used to evaluate the effects of assimilation. Relative to "average" upper, middle, or lower crust, the Crowsnest and Howell Creek samples are enriched in most trace elements aside from P, Ti, Y, and the HREE (Fig. 9). In particular, the high Nd and Sr concentrations in the magmas, relative to crustal values, would require substantial assimilation or contamination to modify isotopic compositions markedly. There are no obvious correlations of either εNd_T or Sr_T with major element concentrations (not plotted).

Post-emplacement alteration of the volcanic rocks is another possible explanation of the scatter in the isotopic data, especially given the metamorphism that the Crowsnest volcanics have experienced (Bégin et al. 1995*b*; Peterson et al. 1997) and the alteration of the Howell Creek suite (Barnes 2002). Such alteration of volcanic rocks should affect the Rb–Sr isotope system more than the Sm–Nd system (e.g., Cousens et al. 1993). If a single end member was responsible for alteration, the data should form a linear array on a plot of Sr_T versus 10^4/Sr. Such is not the case for the Crowsnest samples (Fig. 10, circles), although a stronger case could be made for such an array for the Howell Creek samples (triangles, Fig. 10). Formational waters from the Western Canada Sedimentary Basin are possible proxies for fluids that interacted with the volcanics; these waters have higher $^{87}Sr/^{86}Sr$ but lower Sr concentrations than the volcanics (Fig. 10). The scatter in the data for the volcanics may simply reflect multiple sources of the fluids that interacted with these samples. Another possibility is that the $^{87}Sr/^{86}Sr$ is increased by precipitation of secondary calcite during metamorphism; the lack of a single linear trend in Fig. 10 would then be the product of different sources of carbonate-saturated fluids. It is reasonable to conclude, however, that the wide variation in

Fig. 3. Selected inter-element variation diagrams for Crowsnest samples (circles) and Howell Creek phonolites (upright triangles) and trachytes (inverted triangles).

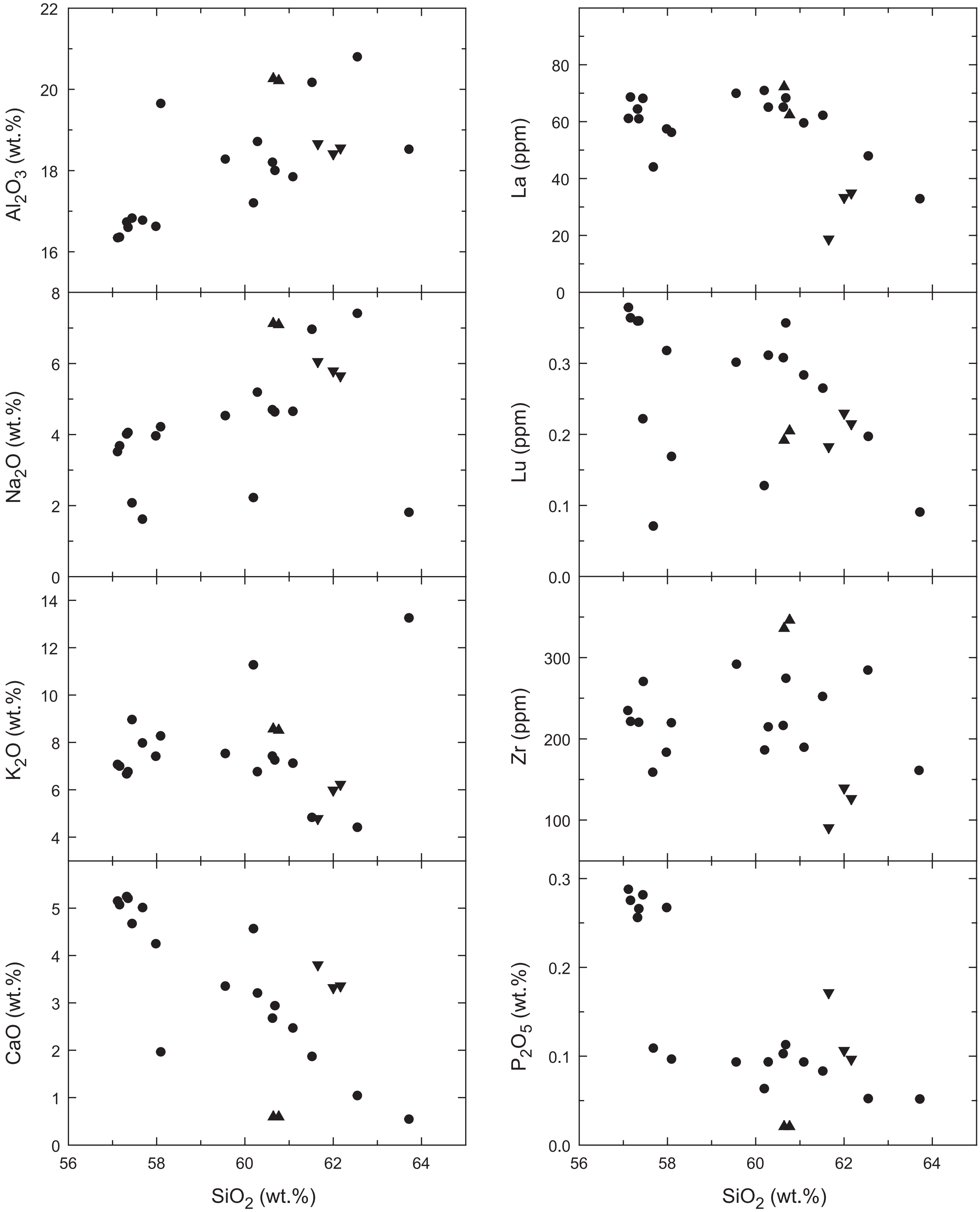

Sr_T measured for the Howell Creek samples, particularly when the datum from Peterson et al. (1997) is included (Sr_T = 0.7096), may result from post-emplacement alteration. This conclusion is supported by both the alteration apparent in thin section and the existence of hydrothermal ore deposits in the area.

Fig. 4. Multi-element diagrams for Crowsnest and Howell Creek samples. Normalized to primitive mantle values of McDonough and Sun (1995). (*a*) Crowsnest samples: latites (squares), phonolites (upright triangles), trachytes (inverted triangles). (*b*) Howell Creek samples: phonolites (upright triangles), trachytes (inverted triangles). Shaded area shows range for Crowsnest samples for comparison.

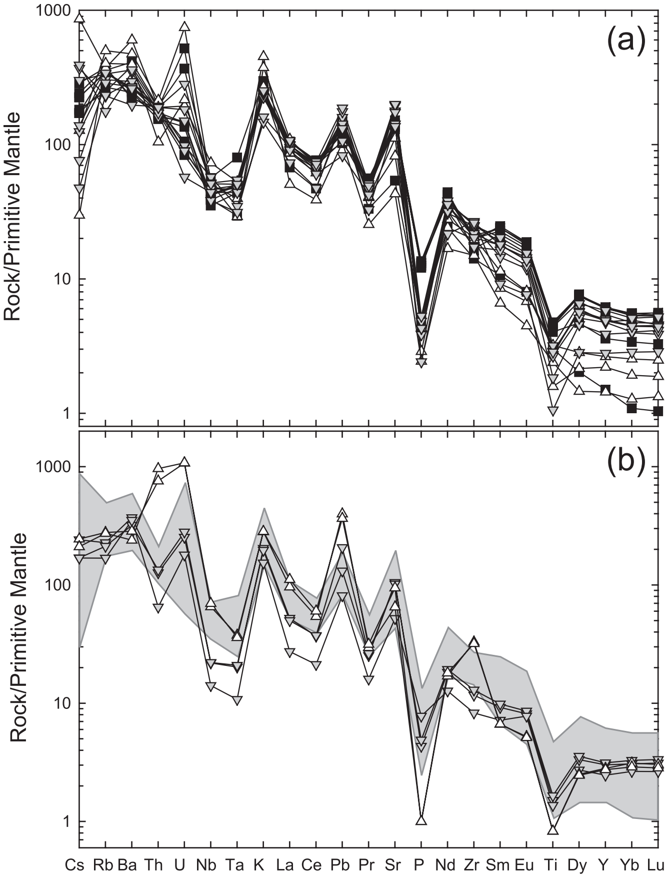

Fig. 5. Chondrite-normalized REE diagrams for Crowsnest and Howell Creek samples. Normalized to CI chondrite values of McDonough and Sun (1995). (*a*) Crowsnest samples (symbols as in Fig. 4*a*). (*b*) Howell Creek samples (symbols as in Fig. 4*b*). For comparison, ranges for Crowsnest trachytes (light shading) and phonolites (dark shading) from Willoughby Ridge are shown.

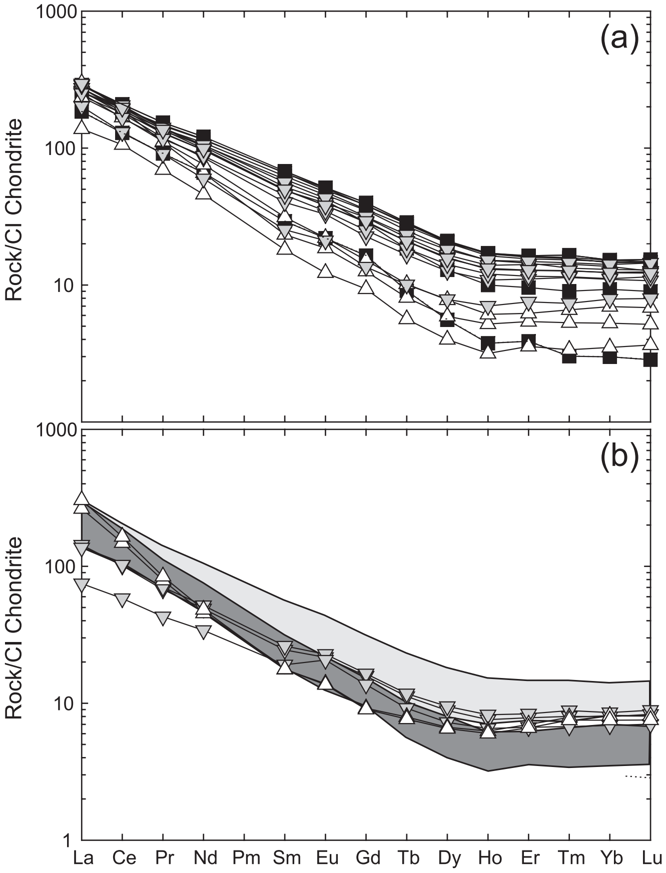

Given the greater mobility of large-ion lithophile elements (LILE) relative to REE in low-temperature metamorphic or hydrothermal fluids (Landoll et al. 1994, and references therein), the Nd system should be less disturbed, so such alteration is unlikely to be able to explain the range in ε_{Nd} observed in these samples. The variation in the εNd_T values, thus, reflects heterogeneities in the source region.

Comparison with other suites

As reviewed by Thompson and Fowler (1986), potassic magmas are produced in three geodynamic settings: (1) rarely in subduction settings, where they are found far from the trench, (2) during and after continental collision, and (3) very rarely in extensional intra-continental igneous settings. Both the Crowsnest and Howell Creek suites have HFSE depletions and LILE enrichments that are commonly attributed to a component of subduction-related fluids in the source region (Tatsumi et al. 1986; Ellam and Hawkesworth 1988). To constrain the possible geodynamic setting better, we compare the trace element geochemistry of these two suites with other suites for which a geodynamic setting has already been proposed or demonstrated.

Whole-rock elemental geochemistry

Multi-elemental, mantle-normalized spidergrams provide an effective means by which to compare the Crowsnest and Howell Creek samples with other suites. The patterns of the samples from the nearby Commerce Mountain area of southeastern British Columbia (Goble et al. 1999) are very similar to those of the Crowsnest and Howell Creek samples (Fig. 11*a*), with depletions in Nb, Ta, P, and Ti relative to neighbouring elements producing a “sawtooth” pattern. In detail, the lower Nb and Ta in the Commerce Mountain samples are more akin to the depletions in the nearby Howell Creek suite, rather than the depletions in the Crowsnest samples. Goble et al. (1999) proposed that the parental magma of the Commerce Mountain suite formed by partial melting of lower continental crust.

The Late Triassic Zippa Mountain intrusion, located in northwest British Columbia, is an alkaline body zoned from marginal clinopyroxenite to a core of syenite (Coulson et al. 1999). These authors proposed that the parental magma was produced in an arc-type setting. The syenites of the Zippa Mountain intrusion tend to plot below the range for the Crowsnest samples (Fig. 11*b*), although they share the same general “sawtooth” pattern marked by low Nb, P, and Ti.

Fig. 6. Initial radiogenic isotope values for Crowsnest (solid circles) and Howell Creek (solid diamonds) samples from this study. Values calculated for 100 Ma; bulk-earth (cross) values calculated with $^{87}Rb/^{86}Sr = 0.085$, present-day $^{87}Sr/^{86}Sr = 0.705$, $^{147}Sm/^{144}Nd = 0.1967$, and present-day $^{143}Nd/^{144}Nd = 0.512638$. Cross marks bulk-earth values. Analytical uncertainty (at 2 SD) is smaller than symbol size. Other data shown: Crowsnest (open circles), Howell Creek (open diamond), and Crowsnest Lake dyke (open upright triangle) from Peterson et al. (1997). Rainy Ridge (open square) and Commerce Mountain (open inverted triangle) from Goble et al. (1999). Data for lower crustal xenoliths from central Montana (x, Joswiak 1992) and from the Snake River Plain (★, Leeman et al. 1985). Two other xenoliths from the Snake River Plain plot off the figure at low ε_{Nd} (< –20) and high $^{87}Sr/^{86}Sr$ (> 0.713). Also shown are fields from other regions of western North America: BCCT (Cretaceous and Tertiary granitoids in British Columbia; Ghosh 1995), CS (Coryell Syenite; Ghosh 1995), MF (Yellow Lake Member of the Marron Formation; Dostal et al. 2003), MR (minettes, Milk River, southern Alberta; Buhlmann et al. 2000), AR (samples from the Absaroka Range, USA; Meen and Eggler 1987; Feeley et al. 2002; Feeley and Cosca 2003). Dashed line encloses range of samples from the alkaline Sunlight Volcano (Feeley and Cosca 2003).

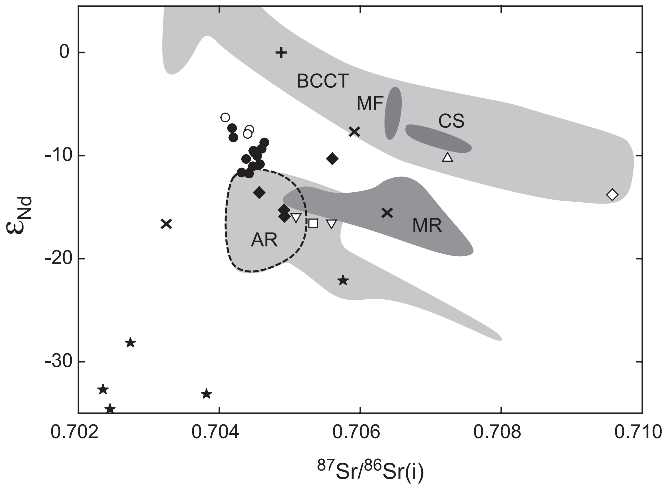

Fig. 7. Plot of K_2O versus Na_2O (in wt.%). Trends after McBirney (1993) and Winter (2001). Solid circles are Crowsnest samples, solid triangles are Howell Creek samples. Outlined fields are for trachytes from both areas (T), trachyandesites (TA) and phonolites (P) from the Crowsnest suite. Howell Creek phonolites are the superimposed triangles labelled P.

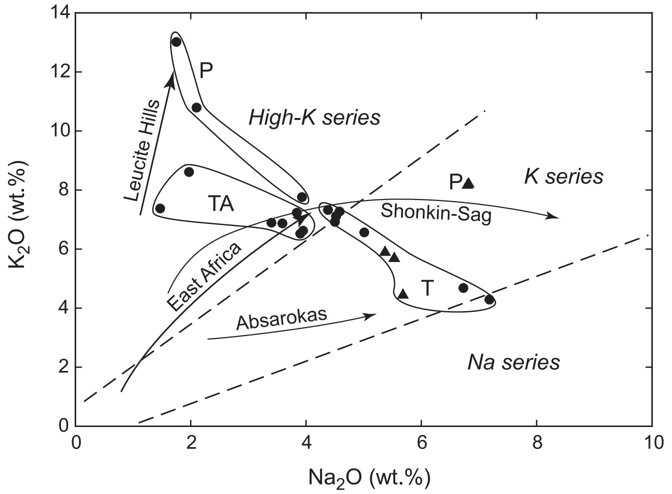

Fig. 8. Initial radiogenic isotope values for Crowsnest samples, differentiated by location. SC, Star Creek; MB, Ma Butte; WR, Willoughby Ridge; RCN, Racehorse Creek (North); RCS, Racehorse Creek (South). RCN and RCS are < 2 km apart. Values calculated for 100 Ma. Cross in lower left is ±2 SD to represent analytical uncertainty.

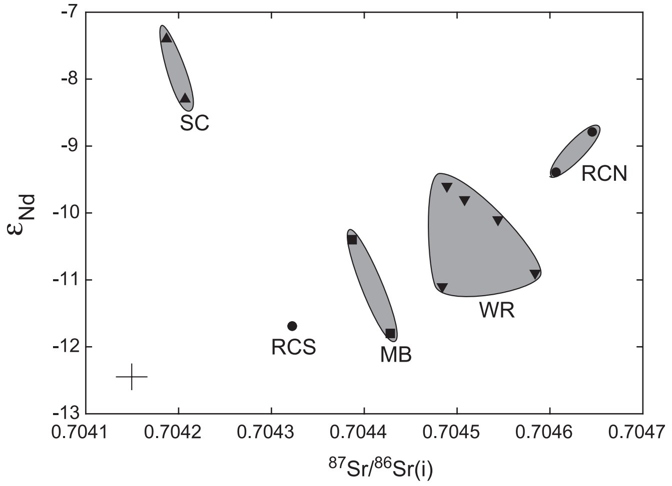

The Eocene-age Penticton Group rocks, which crop out ~340 km west of Howell Creek in British Columbia, contain analcime-bearing mafic volcanic rocks in the Yellow Lake Member of the Marron Formation (Dostal et al. 2003). These rocks plot mostly in the phonotephrite and tephriphonolite fields on the TAS diagram, being more mafic than the Crowsnest or Howell Creek samples. Despite their more mafic nature, the Marron Formation samples are more enriched than the Crowsnest or Howell Creek samples for many trace elements on the multi-element spidergram (Fig. 11*c*). Dostal et al. (2003) proposed an origin of these rocks by partial melting of subcontinental mantle lithosphere that had been metasomatized in a Precambrian subduction setting. Numerous workers have proposed similar models for alkaline rocks of Eocene age in the Montana Alkaline Province (O'Brien et al. 1991, 1995; Buhlmann et al. 2000; Greenough and Kyser 2003).

Indeed, similar "sawtooth" patterns are seen for Eocene-age rocks of the Montana Alkaline Province, with strong similarities of the Crowsnest and Howell Creek samples to latites from the Bearpaw Mountains (Fig. 11*d*; data from Macdonald et al. 1992), samples from the Shonkin Sag (Fig. 11*e*; data from Greenough and Kyser 2003), and latites and trachytes from the Sunlight Volcano, Absaroka Range (Fig. 11*f*; data from Feeley and Cosca 2003). In contrast, the calc-alkaline andesites and dacites from the Washburn center in the Absarokas have different patterns, with less enrichment in Rb, Ba, Th, U, Nb, Ta, and K (Fig. 11*g*; data from Feeley et al. 2002).

Further afield, subduction-related syenites of Siluro-Ordovician age from Scotland studied by Thompson and Fowler (1986) have patterns similar to those of the Crowsnest and Howell Creek suites, albeit with lower Nb and Ta and

Fig. 9. Multi-element diagram showing average values for crustal rocks (data from Rudnick and Gao 2004): circles, upper crust; triangles, middle crust; squares, lower crust; diamonds, whole crust). Shaded area shows range for Crowsnest samples for comparison. Normalized to primitive mantle values of McDonough and Sun (1995).

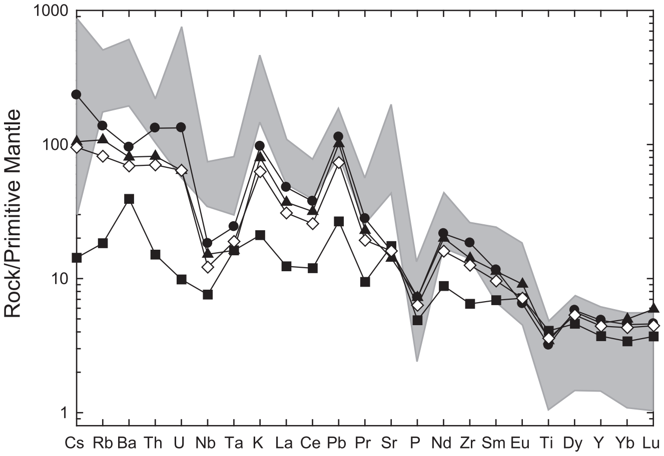

more variable LREE contents (Fig. 11*h*). In contrast, the patterns for silicic members of a rift-related basalt–benmoreite–trachyte suite from the Kenyan Gregory Rift (Baker et al. 1977) are distinctly different (Fig. 11*i*).

Fig. 10. $^{87}Sr/^{86}Sr$ and $10^4/Sr$ values for the Crowsnest (solid circles) and Howell Creek (solid triangles) samples compared with ranges for formational waters from the Western Canadian Sedimentary Basin (Connolly et al. 1990) and seawater at 100 Ma. Not plotted are samples from Upper Cretaceous and Middle Jurassic formations with very low Sr contents. UD, Upper Devonian; M, Mississippian; LJ, Lower Jurassic; LC, Lower Cretaceous. Fields drawn based on data from Connolly et al. (1990). UD and LC fields truncated to maximize spread in Crowsnest and Howell Creek samples; UD extends to $^{87}Sr/^{86}Sr \approx 0.713$; LC extends to $10^4/Sr \approx 100$.

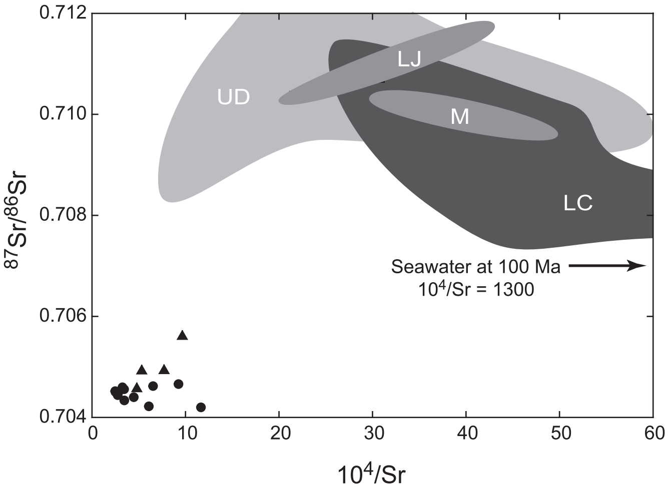

Radiogenic isotopes

The Crowsnest samples are characterized by low εNd_T, reflecting a long-term LREE enrichment (low Sm/Nd) in the source region, but low Sr_T, requiring a near bulk-earth (or lower) time-integrated Rb/Sr. This behaviour contrasts with that of other Cretaceous and Tertiary felsic intrusives (BCCT in Fig. 6; Ghosh 1995), the Eocene analcime-bearing volcanics (MF in Fig. 6; Dostal et al. 2003), or the Coryell Syenite (CS in Fig. 6; Ghosh 1995), all of which crop out further west in British Columbia.

The isotope geochemistry of the Crowsnest and Howell Creek suites is similar to suites from the Montana Alkaline Province to the southeast. The minettes in the Milk River area of southern Alberta (MR in Fig. 6; Buhlmann et al. 2000), and many of the other suites from the Montana Alkaline Province, have similar εNd_T but more radiogenic Sr_T (cf. review in Buhlmann et al. 2000). The volcanics in the Absaroka Range in southern Montana and northern Wyoming have generally lower εNd_T and a wide range of Sr_T, including values as low as those for the Crowsnest and Howell Creek suites (AR in Fig. 6; Meen and Eggler 1987; Feeley et al. 2002; Feeley and Cosca 2003). The lowest values of Sr_T are found in samples from the alkaline Sunlight Volcano (Feeley and Cosca 2003), whereas samples from calc-alkaline centers, such as Washburn Volcano (Feeley et al. 2002) and the Independence volcanic suite (Meen and Eggler 1987), tend to have higher Sr_T and lower εNd_T. Although the similarity of the Crowsnest, Howell Creek, and Sunlight fields may indicate similar source regions, the Sunlight suite contains mafic rocks, unlike the Crowsnest and Howell Creek suites.

Origin of trachyte–phonolite–syenite magmas

The samples of both the Crowsnest and Howell Creek suites are neither over- nor undersaturated in silica, as evidenced by the lack of normative nepheline or quartz in most samples. When projected into the SiO_2–$KAlSiO_4$–$NaAlSiO_4$–H_2O system, these samples lie mostly on the $NaAlSi_3O_8$–$KAlSi_3O_8$ join (Fig. 12), making them syenitic melts, assuming that the whole-rock compositions are reasonable proxies for the liquid compositions. Our suite of Crowsnest samples is biased because we excluded samples of “blairmorite,” the variant of analcime phonolite containing abundant analcime that has been the focus of much earlier study (e.g., Pearce 1967, 1970; Ferguson and Edgar 1978; Peterson and Currie 1993; Bégin et al. 1995*a*; Peterson et al. 1997). These rocks would have normative nepheline and would extend the range of compositions towards the minima (“m”) on the feldspar$_{ss}$–nepheline$_{ss}$ cotectic in Fig. 12. These samples were excluded because previous workers suggested that accumulation of analcime played a role in the genesis of these samples (Pearce 1967; Peterson and Currie 1993). Such crystal accumulation would invalidate the assumption that the whole-rock composition is a reasonable proxy for the original liquid composition.

Although not uncommon, syenitic melts are enigmatic because the feldspar join in this system is a thermal divide between a quartz-saturated minimum, representing granitic liquids, and a nepheline-saturated minimum, representing nepheline syenite liquids. As discussed later in the text, syenitic liquids may be produced by fractional crystallization from a trachybasaltic parent produced by partial melting in the mantle, by direct partial melting in the mantle, or by partial melting in the lower crust.

Experimental studies confirm that alkali-rich basaltic or trachybasaltic liquids can be produced by partial melting of peridotite containing phlogopite or phlogopite and pargasitic

Fig. 11. Multi-element diagrams comparing the range for the Crowsnest samples (shaded area) to other suites. All are normalized to primitive mantle values of McDonough and Sun (1995). (*a*) Mafic, felsic, and porphyritic syenite samples from Commerce Mountain (Goble et al. 1999). (*b*) Syenites from the Late Triassic Zippa Mountain intrusion of northwest British Columbia (Coulson et al. 1999). (*c*) Analcime-bearing mafic volcanics of the Yellow Lake Member of the Marron Formation, south-central British Columbia (Dostal et al. 2003). (*d*) Latites (circles) and felsic minettes (> 57 wt.% SiO_2, diamonds) from the Bearpaw Mountains, Montana (Macdonald et al. 1992). (*e*) Samples from the Shonkin Sag, Montana (Greenough and Kyser 2003). (*f*) Latites and trachytes from the Sunlight Volcano suite, Absaroka Range, Wyoming (Feeley and Cosca 2003). (*g*) Andesites and dacites from Washburn Volcano, Absaroka Range, Wyoming (Feeley et al. 2002). (*h*) Siluro-Ordovician subduction-related syenites from Scotland (Thompson and Fowler 1986). (*i*) Benmoreites and trachytes from a basalt-benmoreite-trachyte suite from the Gregory Rift, Kenya (Baker et al. 1977).

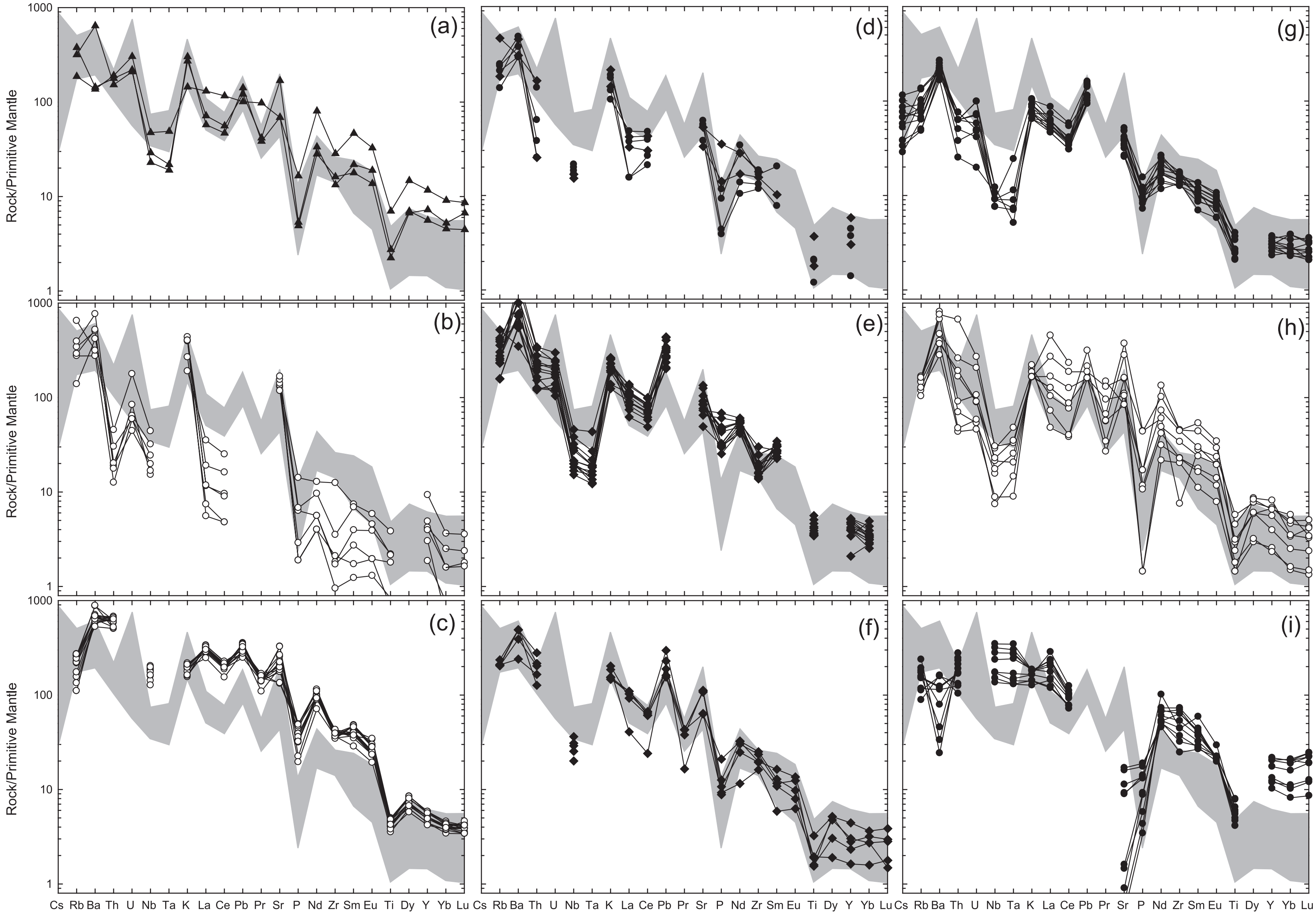

Fig. 12. Compositions of Crowsnest (circles) and Howell Creek (triangles) samples projected into the SiO_2–$NaAlSiO_4$–$KAlSiO_4$ system. Phase relationships illustrated for 0.1 GPa, H_2O-saturated conditions after Fudali (1963) and Hamilton and MacKenzie (1965). Compositions projected using the method of Pearce (1967). Also shown are compositions of latites and trachytes from the alkaline Sunlight Volcano suite, Absaroka Range (open squares, Feeley and Cosca 2003), and of andesites and dacites from the calc-alkaline Washburn Volcano, Absaroka Range (filled squares, Feeley et al. 2002).

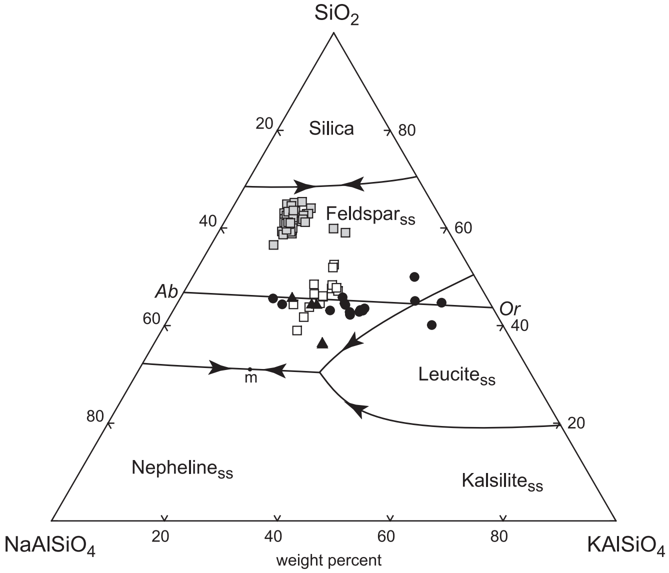

Fig. 13. Total alkalis versus silica diagram comparing the whole-rock compositions of Crowsnest (grey diamonds) and Howell Creek (grey circles) samples to experimental liquids. Triangles: lowest temperature (most alkali- and silica-rich) liquids of Meen (1987) at 1 GPa and 1100–1250 °C (1, his starting composition 2080; 2, composition 2082; 3, composition 2085; 4, composition 2023). Also shown are liquids produced by dehydration melting of an alkali basalt (Kaszuba and Wendlandt 2000). Star, composition of the starting material; circles, the liquid compositions produced at 0.7 GPa with H_2O present (black symbols) and with H_2O + CO_2 (open symbols); squares, liquid compositions produced at 1.0 GPa with H_2O present (closed symbols) or with H_2O + CO_2 (open symbols).

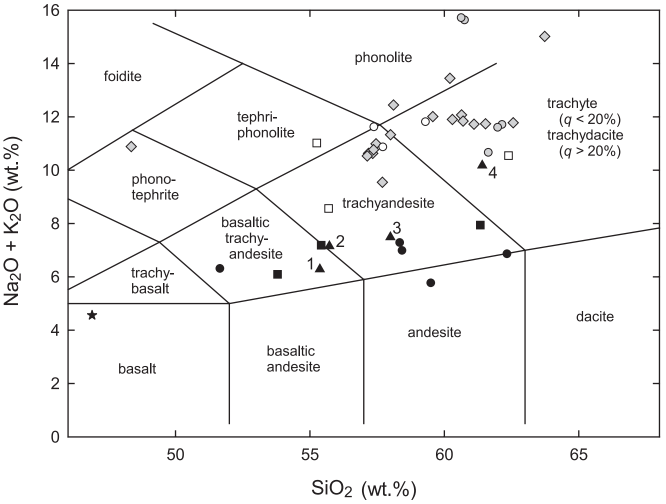

amphibole (e.g., Esperança and Holloway 1987; Tatsumi and Koyaguchi 1989; Hesse and Grove 2003; Conceição and Green 2004). These melts can evolve by fractional crystallization to produce alkaline silicic melts. Meen (1987) demonstrated that equilibrium crystallization of basaltic andesite melts at 1 GPa produces residual basaltic trachyandesite and trachyandesite liquids enriched in K_2O (Fig. 13). Equilibrium crystallization of trachyandesite liquid at the same conditions produced trachyte liquids, albeit less alkaline than the Crowsnest or Howell Creek trachytes (Fig. 13). Nekvasil et al. (2004) experimentally verified that trachybasalt liquids could evolve to trachyandesite and trachyte by fractional crystallization. At lower crustal conditions (~1 GPa), the evolved melts are sodic; at mid-crust conditions (~0.4 GPa), the melts evolve to more potassic compositions; lower pressure (1 atm) produces subalkali evolved melts.

An example of this petrogenesis would be the Sunlight volcanics from the Absaroka field in Wyoming. The silicic members of this suite, which are geochemically and isotopically similar to the Crowsnest and Howell Creek samples, also plot as syenites (Fig. 12), unlike silicic samples from the calc-alkaline Washburn volcanics. It is unlikely that such a scenario applies to either the Crowsnest or Howell Creek suites, because the fractional crystallization paths in both studies involved plagioclase, which should have produced a Eu anomaly in the REE patterns. Such an anomaly is not seen for either suite (Fig. 5). This scenario cannot be ruled out completely because of the mineralogical evidence consistent with differentiation of the Crowsnest magmas at high fO_2 (oxygen fugacity; Luth and Bowerman 2004). Such conditions would increase Eu^{3+}/Eu^{2+} and possibly prevent the substitution of Eu into plagioclase, thereby invalidating the inference that the absence of a Eu anomaly rules out plagioclase fractionation.

Production of alkali silicic melts directly by partial melting of mantle assemblages may produce "syenitic" melts, given that glasses found in mantle xenoliths have a wide range of compositions, with 40–70 wt.% SiO_2, 0–10 wt.% Na_2O and K_2O, and Mg#s of 20–90 (Mg# =100 × molecular MgO/(MgO + FeO^T) (cf. summary by Draper and Green 1997). The low volume and volatile-rich nature of these melts should cause them to freeze upon ascent where the peridotite–H_2O–CO_2 solidus increases in temperature, and hence they should not be emplaced in the upper crust or erupted (cf. Draper and Green 1997, 1999 for discussion). The presence of peridotitic xenoliths in potassic latites in Arizona (Tyner and Smith 1986), however, argues in favour of a direct mantle origin of these rocks. These latites have high Mg# (68–71) and relatively high Ni concentrations (> 200 ppm), which support a mantle source. In contrast, the low Ni concentrations (< 20 ppm) and Mg# (11–30) of the Crowsnest and Howell Creek samples do not support a direct mantle origin.

Foley (1992) advocated a "vein plus wall-rock" model to produce the parental magmas of a variety of alkaline igneous rocks. A subsequent experimental study by Foley et al. (1999) demonstrates that partial melting of "vein" assemblages of clinopyroxene + phlogopite + K-richterite ± ilmenite ± apatite ± rutile at 1.5 GPa produce highly alkaline liquids (volatile-free compositions: 49.3–56.8 wt.% SiO_2, 13.8–18.8 wt.% (Na_2O + K_2O), 9.9–13.9 wt.% K_2O). These liquids, however, are Mg-rich (~8 wt.% MgO) and Al_2O_3-poor (2–5 wt.%), suggesting they could provide at most only part of the source of parental liquids of the Crowsnest and Howell Creek suites.

The final mechanism, partial melting in the lower crust, has been examined extensively. In the system SiO_2–$NaAlSi_3O_8$–$KAlSi_3O_8$–H_2O, increasing pressure shifts the composition of the first-produced (minimum or eutectic) melt away from the quartz apex towards the feldspar sideline, approximately parallel with the SiO_2–$KAlSi_3O_8$ side line (Tuttle and Bowen 1958; W.C. Luth et al. 1964; Huang and Wyllie 1975). Huang and Wyllie (1975, p. 747) suggest that melting at 3 GPa would "…produce an initial liquid with only a few percent normative quartz; it would be more like a syenite than a granite". Ebadi and Johannes (1991) confirmed the shift in the composition of the initial liquid away from the quartz apex. Their liquids still had significant normative quartz (22% at 1 GPa). These workers also found that decreasing aH_2O by dilution with CO_2 shifts the composition of the initial melt to more Or-rich compositions, leaving the quartz content of the liquid unchanged.

In more complex systems, partial melts of a muscovite granite (+5 wt.% H_2O) at 1.5 GPa and 650–1000 °C (Huang and Wyllie 1981) have > 15% normative quartz (Fig. 14). Litvinovsky et al. (2000) conducted experiments on a charnockite (67 wt.% SiO_2, plagioclase + microcline + biotite + quartz + small amounts of amphibole and orthopyroxene) at 1.5, 2.0, and 2.5 GPa. Two series of experiments were conducted, one set in the presence of an H_2O–CO_2 fluid, the other with no added volatiles. In all cases, the melts produced contained 20%–30% normative quartz (Fig. 14). Litvinovsky et al. (2000) concluded that it was impossible to produce a syenitic liquid by partial melting of a quartz + feldspar protolith, even at lower crustal pressures.

The experiments of Meen (1987) discussed earlier in the text may be interpreted in terms of partial melting of basaltic andesite and trachyandesite bulk compositions. The partial melts are not as alkaline as the Crowsnest and Howell Creek samples (Fig. 13). Higher alkali contents may require an additional host for alkalis in the source region, such as phlogopite.

Kaszuba and Wendlandt (2000) produced a range of trachyandesitic to trachytic liquids by dehydration melting in the system alkali basalt–H_2O–CO_2 (Fig. 13). They observed that the liquids become more potassic with increasing XCO_2 (their Fig. 11*b*); but the liquid with the highest K_2O content still had $Na_2O/K_2O > 1$, which is higher than that of the samples from the Crowsnest or Howell Creek suites. This difference may be a result of the composition of their starting material, a natural alkali basalt with 3.33 wt.% Na_2O and 1.15 wt.% K_2O. Whether a more potassic starting composition would produce more potassic liquids under similar conditions is unknown; Kaszuba and Wendlandt's liquids were the most potassic of any produced by partial melting experiments on alkali basalts (cf. their Fig. 11*a*). The liquids produced in the H_2O–CO_2 experiments (shaded triangles in Fig. 14) lie between the quartz-saturated and nepheline-saturated minima in the SiO_2–$NaAlSiO_4$–$KAlSiO_4$ system. If these liquids represent minimum-melt compositions, increasing K_2O in the starting composition would not increase K_2O/Na_2O in the initial melts. This possibility needs to be tested experimentally.

Fig. 14. Compositions of melts produced in partial melting experiments of quartzofeldspathic protoliths. HW, melts produced at 1.5 GPa by partial melting of a muscovite granite in the presence of an H_2O-rich fluid (Huang and Wyllie 1981); L1 and L2, melts produced at 1.5–2.5 GPa by partial melting of a charnockite in the presence of an H_2O–CO_2 fluid (L1) and in the absence of a fluid (L2) (Litvinovsky et al. 2000); KW, melts produced by dehydration melting of alkali basalt with H_2O (KW field) and with H_2O–CO_2 (filled triangles) by Kaszuba and Wendlandt (2000).

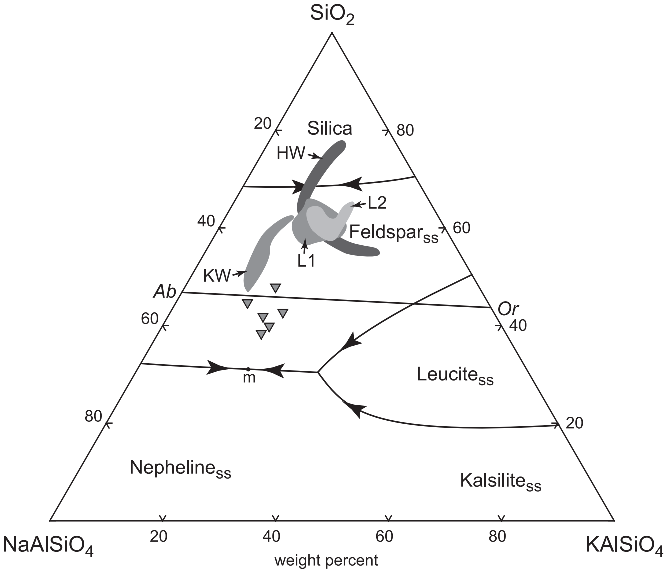

Petrogenetic model

Previous models for the Crowsnest volcanics have the source region in the lower crust (Ferguson and Edgar 1978; Peterson et al. 1997) or possibly in the lithospheric upper mantle (Peterson et al. 1997). As mentioned earlier in the text, Goble et al. (1999) proposed that partial melting of lower continental crust produced the Commerce Mountain magmas. A key issue, therefore, is whether the source region is in the crust or the mantle. As discussed earlier, the major element geochemistry is equally permissive of an origin by fractional crystallization at high fO_2 of an alkalic basalt parent, which would have been formed in the upper mantle or by partial melt of an alkali basalt protolith in the lower crust.

The low values of εNd_T and Sr_T are consistent with a source region that has had a long-term enrichment in LREE (low Sm/Nd) and Rb depletion relative to Sr, such that Rb/Sr is low. This source could be in the lithospheric mantle or in the lower crust. Either is possible; there is indirect evidence for low ε_{Nd} and low $^{87}Sr/^{86}Sr$ lithospheric mantle to the east in the Absaroka field studied by Feeley (2003), who argued for a source region of the alkaline Sunlight Volcano suite in ancient, depleted subcontinental lithospheric mantle that had been subsequently enriched by low Sm/Nd and Rb/Sr metasomatism. He further suggested the discrepancies between the elemental concentrations and isotopic ratios required a more recent metasomatic enrichment event, especially of the LILEs. His geodynamic model generated the parental magmas by "…metasomatism of asthenosphere and subcontinental mantle lithosphere during shallow subduction of the Farallon plate during the Late Cretaceous through Paleocene, followed in the Eocene by foundering of the slab and primary basalt generation through major heating associated with upwelling and influx of hot asthenosphere" (Freeley 2003, p. 329).

On the other hand, there is evidence for crust with low ε_{Nd} and low $^{87}Sr/^{86}Sr$. In their study of the Colville Igneous Complex in northeastern Washington state, ~400 km west of the Crowsnest and Howell Creek localities, Morris et al. (2000) suggested a crustal source with low ε_{Nd} and low $^{87}Sr/^{86}Sr$ was involved in the petrogenesis of the silicic rocks of the Klondike Mountain Formation. They proposed that this source was "ancient lower-crustal rocks that had undergone Rb depletion during granulite facies metamorphism" (Morris et al. 2000, p. 62). They further suggested these rocks were Proterozoic in age and contribute the "subduction signature" of enriched LILE and depleted HFSE to the Colville samples. They reinforced their argument by pointing to lower crustal xenoliths in dykes in Central Montana (Joswiak 1992), 600 km east-southeast of the Colville Igneous Complex. These xenoliths have low $^{87}Sr/^{86}Sr$ and ε_{Nd} (Fig. 6) and had experienced granulite facies metamorphism during the Hudsonian orogeny at ~1.7 Ga. Morris et al. (2000, p. 62) proposed that it "is reasonable to assume such crust might exist beneath northeast Washington". By the same logic, it is equally possible that such crust could be present to the north, providing a source region for the Crowsnest and Howell Creek magmas. Further south, Leeman et al. (1985) sampled crustal xenoliths with low ε_{Nd} and quite variable $^{87}Sr/^{86}Sr$, including a number with very low values (stars, Fig. 6). Partial melting of an alkali basaltic protolith in the lower crust would be consistent with the absence of more mafic magmas that might be expected to be present if fractional crystallization of a mantle-derived magma was responsible for these rocks.

In the southern Canadian Cordillera, the high heat flow has led to models in which asthenospheric upwelling is needed to maintain that heat flow (e.g., Hyndman and Lewis 1999). Further, these authors argue that a thin hot lithosphere beneath the Cordillera was present during Cretaceous and earlier crustal shortening, which implies that asthenospheric upwelling would provide either a heat source for partial melting of hydrous protoliths in the lower crust or in the subcontinental lithospheric mantle that had experienced earlier hydration by metasomatism, possibly from dehydration of the subducting plate, as suggested by Feeley (2003).

Our model for the petrogenesis of the Crowsnest and Howell Creek magmas is consistent with those of previous workers and is similar to those proposed for alkaline igneous rocks of the Montana–Wyoming province. The parental magma was a hydrous alkaline basaltic melt, produced by partial melting primarily of subcontinental lithospheric mantle that had experienced an ancient metasomatic event characterized by low Sm/Nd and Rb/Sr and a subsequent recent metasomatic event, possibly related to dehydration of the subducting Farallon plate. The potassic character of the magmas would thus have resulted from the breakdown of potassic hydrous phases, such as phlogopite and (or) potassic amphibole. Asthenospheric upwelling provided the heat source for the partial melting. Whether the parental melts were produced in a single stage, by partial melting of the mantle, or in two stages, where the basaltic melt ponded and crystallized at the base of the crust and then was itself partially melted to produce trachyandesitic to phonolitic melts, cannot be resolved with the present data, although the absence of more mafic rocks is more consistent with the latter model. Fractional crystallization then produced the more evolved magmas; such crystallization occurred at high pressures, which is consistent with the presence of analcime as a primary phenocryst phase (see discussions in Pearce 1970; Ferguson and Edgar 1978; Peterson et al. 1997; Luth and Bowerman 2004).

The differences in the isotope and trace element geochemistry between the Crowsnest and Howell Creek suites are sufficient to make it unlikely that these suites are in fact genetically related, although they would share a common petrogenetic origin.

Acknowledgements

This paper is based on the undergraduate theses of Melissa Bowerman and Amy Christianson. This research was funded by a National Sciences and Engineering Research Council of Canada (NSERC) Undergraduate Student Research Award to Bowerman, and by NSERC Discovery Grants to Luth and Creaser. The Radiogenic Isotope Facility at the University of Alberta is funded in part by a NSERC Major Facilities Access Grant. We gratefully acknowledge assistance in the field by Brent Gonek (Crowsnest) and Elspeth Barnes (Howell Creek), and in the laboratory by Mark Labbe, Stacey Hagen, and Sergei Matveev. We thank the two anonymous reviewers for their constructive reviews, Associate Editor John Greenough for his editorial input and handling of this manuscript, and the Editor for his patience during our revisions.

References

Baker, B.H., Goles, G.G., Leeman, W.P., and Lindstrom, M.M. 1977. Geochemistry and petrogenesis of a basalt–benmoreite–trachyte suite from southern part of Gregory Rift, Kenya. Contributions to Mineralogy and Petrology, **64**: 303–332.

Barnes, E.M. 2002. The Howell Creek suite, southeastern British Columbia: mid Cretaceous alkalic intrusions and related gold deposition in the Canadian Cordillera. M.Sc. thesis, University of Alberta, Edmonton, Alta.

Bégin, N.J., Beiersdorfer, R.E., and Ghent, E.D. 1995*a*. Mineralogical and geochemical analyses and economic potential of the Crowsnest volcanics. *In* Current research 1995-E. Geological Survey of Canada, pp. 11–25.

Bégin, N.J., Ghent, E.D., and Beiersdorfer, R.E. 1995*b*. Low-temperature metamorphism of the Crowsnest Volcanic Suite, southwestern Alberta. Canadian Mineralogist, **33**: 973–983.

Buhlmann, A.L., Cavell, P., Burwash, R.A., Creaser, R.A., and Luth, R.W. 2000. Minette bodies and cognate mica-clinopyroxenite xenoliths from the Milk River area, southern Alberta: records of a complex history of the northernmost part of the Archean Wyoming craton. Canadian Journal of Earth Sciences, **37**: 1629–1650.

Conceição, R.V., and Green, D.H. 2004. Derivation of potassic (shoshonitic) magmas by decompression melting of phlogopite plus pargasite lherzolite. Lithos, **72**: 209–229.

Connolly, C.A., Walter, L.M., Baadsgaard, H., and Longstaffe, F.J. 1990. Origin and evolution of formation waters, Alberta Basin, Western Canada Sedimentary Basin. II. Isotope systematics and water mixing. Applied Geochemistry, **5**: 397–413.

Coulson, I.M., Russell, J.K., and Dipple, G.M. 1999. Origins of the Zippa Mountain pluton: a late Triassic, arc-derived, ultrapotassic magma from the Canadian Cordillera. Canadian Journal of Earth Sciences, **36**: 1415–1434.

Cousens, B.L., Spera, F.J., and Dobson, P.F. 1993. Post-eruptive alteration of silicic ignimbrites and lavas, Gran Canaria, Canary Islands: Strontium, neodymium, lead, and oxygen isotopic evidence. Geochimica et Cosmochimica Acta, **57**: 631–640.

Creaser, R.A., Erdmer, P., Stevens, R.A., and Grant, S.L. 1997. Tectonic affinity of Nisutlin and Anvil assemblage strata from the Teslin tectonic zone, northern Canadian Cordillera: Constraints from neodymium isotope and geochemical evidence. Tectonics, **16**: 107–121.

Crook, K.A.W. 1962. Alkali-feldspars from the Crowsnest volcanics, Alberta. Canadian Mineralogist, **7**: 253–263.

Dawson, G.M. 1886. Preliminary report on the physical and geological features of that portion of the Rocky Mountains between latitudes 49° and 51°30′. Geological and Natural History Survey of Canada, Annual Report.

Dostal, J., Breitsprecher, K., Church, B.N., Thorkelson, D., and Hamilton, T.S. 2003. Eocene melting of Precambrian lithospheric mantle: Analcime-bearing volcanic rocks from the Challis–Kamloops belt of south central British Columbia. Journal of Volcanology and Geothermal Research, **126**: 303–326.

Draper, D.S., and Green, T.H. 1997. *P–T* phase relations of silicic, alkaline, aluminous mantle-xenolith glasses under anhydrous and C–O–H fluid-saturated conditions. Journal of Petrology, **38**: 1187–1224.

Draper, D.S., and Green, T.H. 1999. *P–T* phase relations of silicic, alkaline, aluminous liquids: new results and applications to mantle melting and metasomatism. Earth and Planetary Science Letters, **170**: 255–268.

Ebadi, A., and Johannes, W. 1991. Beginning of melting and composition of first melts in the system Qz–Ab–Or–H_2O–CO_2. Contributions to Mineralogy and Petrology, **106**: 286–295.

Ellam, R.M., and Hawkesworth, C.J. 1988. Elemental and isotopic variations in subduction related basalts — Evidence for a three component model. Contributions to Mineralogy and Petrology, **98**: 72–80.

Esperança, S., and Holloway, J.R. 1987. On the origin of some mica-lamprophyres: experimental evidence from a mafic minette. Contributions to Mineralogy and Petrology, **95**: 207–216.

Feeley, T.C. 2003. Origin and tectonic implications of across-strike geochemical variations in the Eocene Absaroka volcanic province, United States. Journal of Geology, **111**: 329–346.

Feeley, T.C., and Cosca, M.A. 2003. Time vs. composition trends of magmatism at Sunlight volcano, Absaroka volcanic province, Wyoming. Geological Society of America Bulletin, **115**: 714–728.

Feeley, T.C., Cosca, M.A., and Lindsay, C.R. 2002. Petrogenesis and implications of calc-alkaline cryptic hybrid magmas from Washburn Volcano, Absaroka Volcanic Province, USA. Journal of Petrology, **43**: 663–703.

Ferguson, L.J., and Edgar, A.D. 1978. Petrogenesis and origin of analcime in volcanic rocks of the Crowsnest Formation, Alberta. Canadian Journal of Earth Sciences, **15**: 69–77.

Floyd, P.A., and Winchester, J.A. 1975. Magma type and tectonic setting discrimination using immobile elements. Earth and Planetary Science Letters, **27**: 211–218.

Foley, S. 1992. Vein-plus-wall-rock melting mechanisms in the lithosphere and the origin of potassic alkaline magmas. Lithos, **28**: 435–453.

Foley, S.F., Musselwhite, D.S., and van der Laan, S.R. 1999 Melt compositions from ultramafic vein assemblages in the lithospheric mantle; a comparison of cratonic and non-cratonic settings. *In* Proceedings of the VIIth International Kimberlite Conference, University of Cape Town, South Africa, April 11–17, 1998, Vol. 1: The J.B. Dawson Vol. *Edited by* J.J. Gurney, J.L. Gurney, M.D. Pascoe, and S.H. Richardson. Red Roof Design, Cape Town, South Africa, pp. 238–246.

Fudali, R.F. 1963. Experimental studies bearing on the origin of pseudoleucite and associated problems of alkalic rock systems. Geological Society of America Bulletin, **74**: 1101–1126.

Ghosh, D.K. 1995. Nd–Sr isotopic constraints on the interactions of the Intermontane Superterrane with the western edge of North America in the southern Canadian Cordillera. Canadian Journal of Earth Sciences, **32**: 1740–1758.

Goble, R.J., Treves, S.B., and Ghazi, A.M. 1993. Comparison of the Rainy Ridge analcime phonolite sill and the Crowsnest Volcanics, Alberta, Canada. Canadian Journal of Earth Sciences, **30**: 1644–1649.

Goble, R.J., Treves, S.B., and Murray, V.M. 1999. Cretaceous intrusions in the Commerce Mountain and adjacent areas of southeastern British Columbia and southwestern Alberta. Canadian Journal of Earth Sciences, **36**: 1939–1956.

Greenough, J.D., and Kyser, T.K. 2003. Contrasting Archean and Proterozoic lithospheric mantle: isotopic evidence from the Shonkin Sag sill (Montana). Contributions to Mineralogy and Petrology, **145**: 169–181.

Hamilton, D.L., and Mackenzie, W.S. 1965. Phase-equilibrium studies in the system $NaAlSiO_4$ (nepheline)–$KAlSiO_4$ (kalsilite)–SiO_2–H_2O. Mineralogical Magazine, **34**: 214–231.

Hesse, M., and Grove, T.L. 2003. Absarokites from the western Mexican Volcanic Belt: constraints on mantle wedge conditions. Contributions to Mineralogy and Petrology, **146**: 10–27.

Holmden, C., Creaser, R.A., Muehlenbachs, K., Bergstrom, S.M., and Leslie, S.A. 1996. Isotopic and elemental systematics of Sr and Nd in 454 Ma biogenic apatites: Implications for paleoseawater studies. Earth and Planetary Science Letters, **142**: 425–437.

Huang, W.L., and Wyllie, P.J. 1975. Melting reactions in the system $NaAlSi_3O_8$–$KAlSi_3O_8$–SiO_2 to 35 kilobars, dry and with excess water. Journal of Geology, **83**: 737–748.

Huang, W.L., and Wyllie, P.J. 1981. Phase relationships of S-type granite with H_2O to 35 Kbar; muscovite granite from Harney Peak, South Dakota. Journal of Geophysical Research, **86**: 515–529.

Hyndman, R.D., and Lewis, T.J. 1999. Geophysical consequences of the Cordillera–Craton thermal transition in southwestern Canada. Tectonophysics, **306**: 397–422.

Joswiak, D. 1992. Composition and evolution of the lower crust, central Montana: evidence from granulite xenoliths. M.Sc. thesis, University of Washington, Seattle, Wash., USA.

Kaszuba, J.P., and Wendlandt, R.F. 2000. Effect of carbon dioxide on dehydration melting reactions and melt compositions in the lower crust and the origin of alkaline rocks. Journal of Petrology, **41**: 363–386.

Landoll, J.D., Foland, K.A., and Henderson, C.M.B. 1994. Nd Isotopes demonstrate the role of contamination in the formation of coexisting quartz and nepheline syenites at the Abu-Khruq Complex, Egypt. Contributions to Mineralogy and Petrology, **117**: 305–329.

Le Maitre, R.W. 2002. Igneous Rocks: IUGS classification and glossary: recommendations of the International Union of Geological Sciences, Subcommission on the systematics of igneous rocks. 2nd ed. Cambridge University Press, Cambridge, UK.

Leeman, W.P., Menzies, M.A., Matty, D.J., and Embree, G.F. 1985. Strontium, neodymium and lead isotopic compositions of deep crustal xenoliths from the Snake River Plain: evidence for Archean basement. Earth and Planetary Science Letters, **75**: 354–368.

Litvinovsky, B.A., Steele, I.M., and Wickham, S.M. 2000. Silicic magma formation in overthickened crust: Melting of charnockite and leucogranite at 15, 20 and 25 kbar. Journal of Petrology, **41**: 717–737.

Luth, R.W., and Bowerman, M. 2004. Microtextural and powder-diffraction study of analcime phenocrysts in volcanic rocks of the Crowsnest Formation, southern Alberta, Canada. Canadian Mineralogist, **42**: 897–903.

Luth, W.C., Tuttle, O.F., and Jahns, R.H. 1964. The granite system at pressures of 4 to 10 kilobars. Journal of Geophysical Research, **69**: 759–773.

Macdonald, R., Upton, B.G.J., Collerson, K.D., Hearn, B.C., and James, D. 1992. Potassic mafic lavas of the Bearpaw Mountains, Montana: mineralogy, chemistry, and origin. Journal of Petrology, **33**: 305–346.

McBirney, A.R. 1993. Igneous Petrology. 2nd ed. Jones and Bartlett, Boston, Mass., USA.

McDonough, W.F., and Sun, S.S. 1995. The composition of the Earth. Chemical Geology, **120**: 223–253.

Meen, J.K. 1987. Formation of shoshonites from calcalkaline basalt magmas: geochemical and experimental constraints from the type locality. Contributions to Mineralogy and Petrology, **97**: 333–351.

Meen, J.K., and Eggler, D.H. 1987. Petrology and geochemistry of the Cretaceous Independence Volcanic Suite, Absaroka Mountains, Montana: clues to the composition of the Archean sub-Montanan mantle. Geological Society of America Bulletin, **98**: 238–247.

Middelburg, J.J., van der Weijden, C.H., and Woittiez, J.R.W. 1988. Chemical processes affecting the mobility of major, minor and trace elements during weathering of granitic rocks. Chemical Geology, **68**: 253–273.

Morris, G.A., Larson, P.B., and Hooper, P.R. 2000. ‘Subduction style’ magmatism in a nonsubduction setting: the Colville Igneous Complex, NE Washington State, USA. Journal of Petrology, **41**: 43–67.

Nekvasil, H., Dondolini, A., Horn, J., Filiberto, J., Long, H., and Lindsley, D.H. 2004. The origin and evolution of silica-saturated alkalic suites: an experimental study. Journal of Petrology, **45**: 693–721.

Norris, D.K. 1964. The Lower Cretaceous of the southeastern Canadian Cordillera. Bulletin of Canadian Petroleum Geology, **12**: 512–535.

O’Brien, H.E., Irving, A.J., and McCallum, I.S. 1991. Eocene potassic magmatism in the Highwood Mountains, Montana: petrology, geochemistry, and tectonic implications. Journal of Geophysical Research, **96**: 13 237 –13 260.

O’Brien, H.E., Irving, A.J., McCallum, S., and Thirlwall, M.F. 1995. Strontium, neodymium, and lead isotopic evidence for the interaction of post-subduction asthenospheric potassic mafic magmas of the Highwood Mountains, Montana, USA, with ancient Wyoming Craton lithospheric mantle. Geochimica et Cosmochimica Acta, **59**: 4539–4556.

Pearce, J.A., and Cann, J.R. 1973. Tectonic Setting of Basic Volcanic-Rocks Determined Using Trace-Element Analyses. Earth and Planetary Science Letters, **19**: 290–300.

Pearce, T.H. 1967. The analcite-bearing volcanic rocks of the Crowsnest Formation. Ph.D. thesis, Queen’s University, Kingston, Ont.

Pearce, T.H. 1970. The analcite-bearing volcanic rocks of the Crowsnest Formation, Alberta. Canadian Journal of Earth Sciences, **7**: 46–66.

Peterson, T.D., and Currie, K.L. 1993. Analcite-bearing igneous rocks from the Crowsnest Formation, southwestern Alberta. *In* Current research, part B. Geological Survey of Canada, Paper 93-1B, pp. 51–56.

Peterson, T.D., Currie, K.L., Ghent, E.D., Bégin, N.J., and Beiersdorfer, R.E. 1997. Petrology and economic geology of the Crowsnest volcanics, Alberta. *In* Exploring for minerals in Alberta: Geological Survey of Canada geoscience contributions, Canada–Alberta Agreement on Mineral Development (1992–1995). *Edited by* R.W. Macqueen. Geological Survey of Canada, Bulletin 500, pp. 163–184.

Price, R.A. 1959. Flathead, British Columbia and Alberta. Geological Survey of Canada, Map 1-1959, scale 1 : 50 000.

Price, R.A. 1962. Fernie Map-Area, East half, Alberta and British Columbia. Geological Survey of Canada, Paper 61-24.

Rudnick, R.L., and Gao, S. 2004. The composition of the continental crust. *In* Treatise on geochemistry, Vol. 3. The Crust. *Edited by* R.L. Rudnick. Elsevier-Pergamon, Oxford, UK, Chap. 1.

Shand, S.J. 1927. The eruptive rocks. John Wiley, New York, N.Y.

Tatsumi, Y., and Koyaguchi, T. 1989. An absarokite from a phlogopite Iherzolite source. Contributions to Mineralogy and Petrology, **102**: 34–40.

Tatsumi, Y., Hamilton, D.L., and Nesbitt, R.W. 1986. Chemical characteristics of fluid phase released from a subducted lithosphere and origin of arc magmas: evidence from high-pressure experiments and natural rocks. Journal of Volcanology and Geothermal Research, **29**: 293–309.

Thompson, R.N., and Fowler, M.B. 1986. Subduction-related shoshonitic and ultrapotassic magmatism: a study of Siluro-Ordovician syenites from the Scottish Caledonides. Contributions to Mineralogy and Petrology, **94**: 507–522.

Tuttle, O.F., and Bowen, N.L. 1958. Origin of granite in light of experimental studies in the system $NaAlSi_3O_8$–$KAlSi_3O_8$–SiO_2–H_2O.

Tyner, G.N., and Smith, D. 1986. Peridotite xenoliths in silica-rich, potassic latite from the transition zone of the Colorado Plateau in north-central Arizona. Contributions to Mineralogy and Petrology, **94**: 63–71.

Winter, J.D. 2001. An introduction to igneous and metamorphic petrology. Prentice-Hall, Inc., Upper Saddle River, NJ.

Wood, D.A., Gibson, I.L., and Thompson, R.N. 1976. Elemental mobility during zeolite facies metamorphism of the Tertiary basalts of eastern Iceland. Contributions to Mineralogy and Petrology, **55**: 241–254.